

*Grzegorz Żabiński, Mateusz Biborski, Marcin Biborski,  
Janusz Stepiński, Ewelina A. Miśta-Jakubowska*

## A LATE MEDIEVAL OR EARLY MODERN FERROUS HACKBUT BARREL FROM THE COLLECTION OF THE CASTLE MUSEUM IN MALBORK

Abstract:

G. Żabiński, M. Biborski, M. Biborski, J. Stepiński, E. A. Miśta-Jakubowska 2018, A Late Medieval or Early Modern ferrous hackbut barrel from the collection of the Castle Museum in Malbork, AMM XIV: 175-212

The paper discusses a ferrous hackbut barrel stored in the collection of the Castle Museum in Malbork. The barrel was perhaps made in the late 15<sup>th</sup> or early 16<sup>th</sup> century, although it may have remained in use much later on. Technological analyses demonstrate that it was forged from semi-hard bloomery steel. During the process of manufacture the metal was overheated, which had a negative impact on utilitarian quality of the barrel. In the Appendix it was attempted at verifying the smelting method with the use of slag inclusion analysis. It seems to confirm that the metal was obtained in the bloomery process.

Key words: 15<sup>th</sup>-17<sup>th</sup> centuries, military, hand-held firearms, hackbut, Castle Museum in Malbork, archaeometallurgy, slag inclusion analysis

Received: 22.10.2017; Accepted: 22.07.2018; Revised: 11.11.2018

### **Introduction**

The aim of this paper is to discuss a ferrous hackbut barrel stored in the collection of the Castle Museum in Malbork (inv. No. MZM/421/MT). Almost nothing can be said on its provenance – the Museum's inventory card says that it came to the collection in result of a purchase. This implies that it was not part of the pre-WWII collection of arms and armour kept at the Castle and it was acquired after 1945.

### **Description and metrical data**

The barrel is a massive tube which slightly narrows at its central part and then broadens again near the muzzle (Fig. 1:1 and 1:5). The overall state of preservation of the artefact is fairly good, save some corrosion pits on the surface. The cross-section of the barrel is round (Fig. 1:2). In its front part the barrel is provided with a sturdy hook which has a round opening in its base (Fig. 1:1). The hook seems to have been forge-welded to the barrel. Near the breech there is a small catch, also provided with a round opening. This catch and the opening in the hook were certainly used for mounting the barrel in its stock, as it is

demonstrated by iconographic examples (see below). The same function was perhaps fulfilled by a small tang in the bottom of the breech (Fig. 1:1 and 1:3). On the right side (from the point of view of a gunner operating the weapon) of the barrel near its end there is a rectangular hollowing which originally served to attach the priming pan. In the end part of this hollowing a round touch hole can be seen (Fig. 1:3). In the front part of the artefact, ca. 10 cm from the muzzle, there is a pair of grooves going in perpendicular to the longer axis of the barrel. It seems that these grooves may have originally gone around the entire circumference of the artefact (Fig. 1:4). An analogous pair of grooves can be seen ca. 27 cm from the end of the barrel (Fig. 1:5). It can be supposed that these grooves had a purely decorative function. Furthermore, a small oblong and partially preserved protrusion can be seen near the muzzle. It may have originally been a foresight. Apart from that, there is a ca. 2 cm long I-shaped hollowing near the muzzle (some sort of a mark?) (Fig. 1:4). On the entire surface of the barrel there are traces of hammering, which suggest that the barrel was forged.



Fig. 1. Hackbut barrel, Castle Museum in Malbork (Inv. No. MZM/421/MT): 1 – general view; 2 – front view of the muzzle; 3 – breech and the touch hole; 4 – side view of the muzzle; 5 – central part. *Photo by G. Żabiński.*

Ryc. 1. Lufa hakownicy, Muzeum Zamkowe w Malborku (nr inw. MZM/421/MT): 1 – widok ogólny; 2 – wylot lufy z przodu; 3 – tylna część lufy z otworem zapłonowym; 4 – boczna strona wylotu lufy; 5 – część środkowa. *Fot. G. Żabiński.*

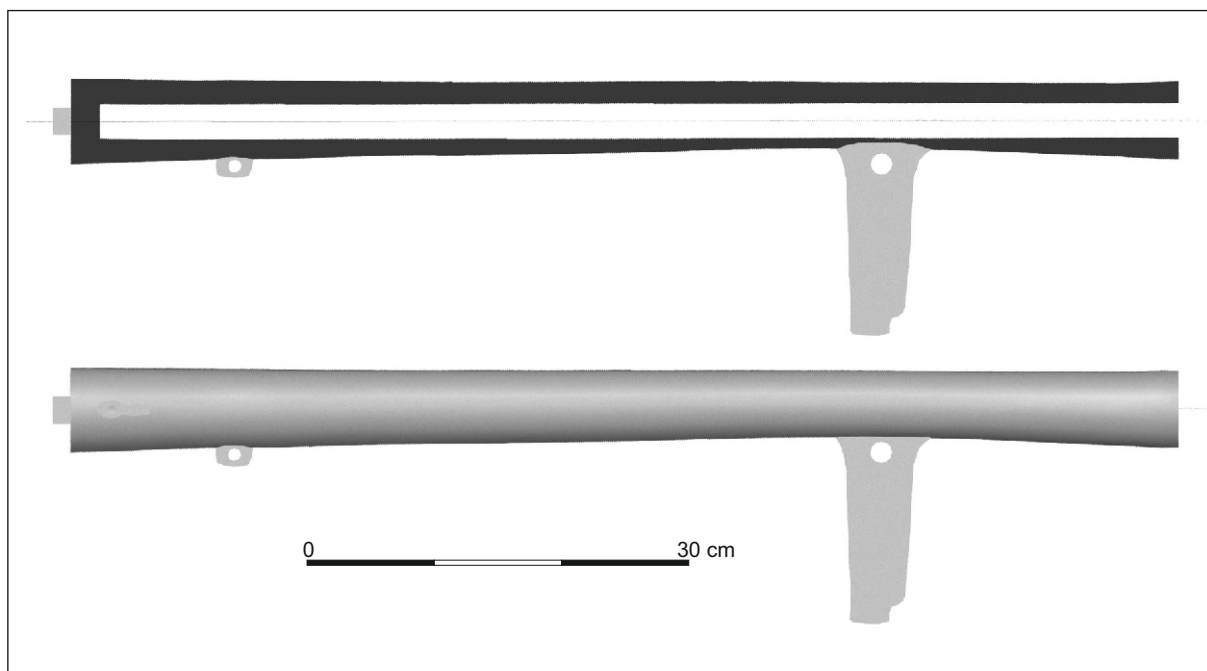


Fig. 2. 3D reconstruction with a cross-section of hackbut barrel from Castle Museum in Malbork. *Elaborated by G. Żabiński.*

Ryc. 2. Rekonstrukcja 3D lufy hakownicy z Muzeum Zamkowego w Malborku wraz z przekrojem. *Oprac. G. Żabiński.*

A 3D reconstruction of the barrel and its cross-section (Fig. 2) suggests a very important trait of the gun. Assuming that the bore goes more or less in parallel to the longitudinal axis of the barrel (as implied by the muzzle's front view, see Fig. 1:2), it can be seen in the cross-section that the barrel's walls are of very uneven thickness. This is especially notable in the lower part of the barrel near the hook, where the wall is almost two times thinner than in the upper part. To some degree, this fact may have been caused by, e.g., difficulties encountered by the manufacturer in the process of forge-welding of the hook to the barrel. This trait, in combination with imperfections of metallurgical nature (see below), in all probability rendered the barrel prone to damage.

The position of the touch hole, which is located on the right side of the barrel is very significant. It is noteworthy that in the earliest examples of hand-held firearms (14<sup>th</sup> – early 15<sup>th</sup> century) the touch hole is usually located on the top or upper part of the breech. This rendered aiming difficult, as smoke and fire from the touch hole significantly impeded the shooter's view. Later on, around the mid-15<sup>th</sup> century, the touch hole was moved to the side of the barrel to eliminate this difficulty<sup>1</sup> (Konieczny 1964, 184-186, Pl. V; Strzyż 2011, 23, 42, 45; 2014, 54-56;

see also Маковская 1992, 16-17, 29). Furthermore, P. Strzyż says that in 16<sup>th</sup> century hackbut barrels the touch hole is located on the side of the weapon at a right angle in relation to the axis of the gun (Strzyż 2011, 23). This seems to be the case concerning the discussed hackbut.

#### Metrical data:

- total weight: 12540 g (12.54 kg)
- total length: 858 mm
- internal length of the barrel: 807 mm
- external diameter of the barrel: 60 mm
- internal diameter of the barrel (calibre): 27 mm
- thickness of the barrel's walls at the muzzle: 16 mm
- distance between the hook and the muzzle: 187 mm
- width of the hook at the base: 60 mm
- width of the hook at the end: 32 mm
- length of the hook: 142 mm
- thickness of the hook: 10.5 mm
- distance between the catch and the muzzle: 705 mm
- width of the catch: 27 mm
- length of the catch: 13.5 mm
- length of the knob at the back of the barrel: 21 mm
- width of the knob at the back of the barrel: 24 mm
- thickness of the knob at the end of the barrel: 14 mm
- distance between the touch hole and the back of the barrel: 34 mm
- diameter of the touch hole: 10 mm

<sup>1</sup> On the other hand, M. Głosek assumes that this occurred as early as ca. 1400 (Głosek 1990, 158); M. Mielczarek is of a similar opinion (see Mielczarek 1998, 62).

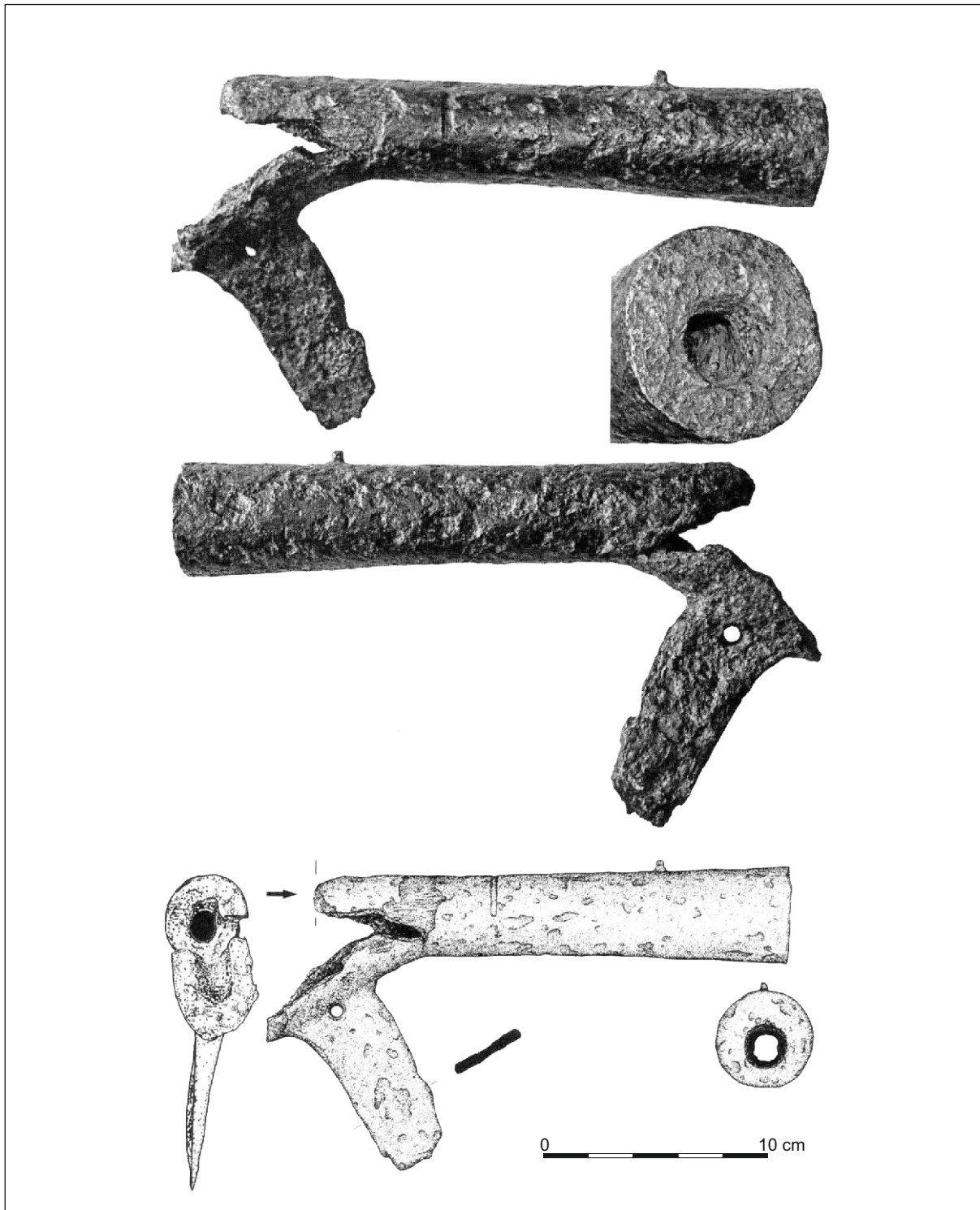


Fig. 3. Fragment of a burst hackbut from Helfštýn Castle in Bohemia (after Figel' *et al.* 2010, 479, Figs. 2, 3:a).

Ryc. 3. Fragment rozerwanej hakownicy z zamku Helfštýn w Czechach (wg Figel' *et al.* 2010, 479, Figs. 2, 3:a).

### Chronology and possible analogies

According to the Museum's inventory card, the barrel is of European provenance and it can be dated to the turn of the 15<sup>th</sup> and 16<sup>th</sup> centuries. Furthermore, the Museum's inventory card mentions

two artefacts from the collection of the Polish Army Museum in Warszawa as very close analogies (Inv. Nos. MWP 298 and MWP 299). It says that similarities include the following traits: the fact that the barrels broaden toward their muzzles;

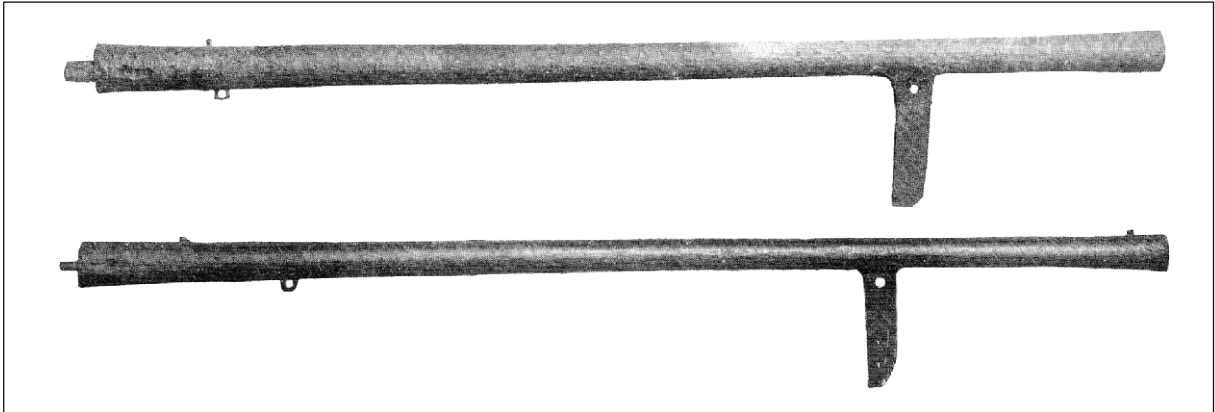


Fig. 4. Two hackbuts from the collection of the National Museum in Prague (after Figel' et al. 2010, 482, Fig. 7).

Ryc. 4. Dwie hakownice ze zbiorów Muzeum Narodowego w Pradze (wg Figel' et al. 2010, 482, Fig. 7).



Fig. 5. Hackbuts in "Zeugbuch", ca. 1502: 1 – brass hackbuts in stocks with heavy butts. Pegs attaching the stocks to the barrels can be seen; 2 – Firing a heavy iron-forged hackbut with a slow match. A priming pan can be seen on the right side of the breech (1 – after *Zeugbuch*, fol. 72v; 2 – after *Zeugbuch*, fol. 73r; Copyright Bayerische Staatsbibliothek München).

Ryc. 5. Hakownice w „Zeugbuch”, ok. 1502: 1 – mosiężne hakownice w łożach z ciężkimi kolbami. Widoczne są kołki mocujące łoża do luf; 2 – strzelanie z ciężkiej hakownicy z kutego żelaza za pomocą lontu. Po prawej stronie tylnej części lufy widoczna panewka (1 – wg *Zeugbuch*, fol. 72v; 2 – wg *Zeugbuch*, fol. 73r; Copyright Bawarska Biblioteka Państwowa, Monachium).

hooks with openings, touch holes on the right side of the breech; tangs at the ends of the barrels; and double grooves near the muzzles and in the central parts of the barrel.

Upon closer inspection, however, these two guns do not seem to offer very convenient analogies. With regard to inv. No. MWP 298 (dated to ca. 1500-1510), general dimensions and the weight

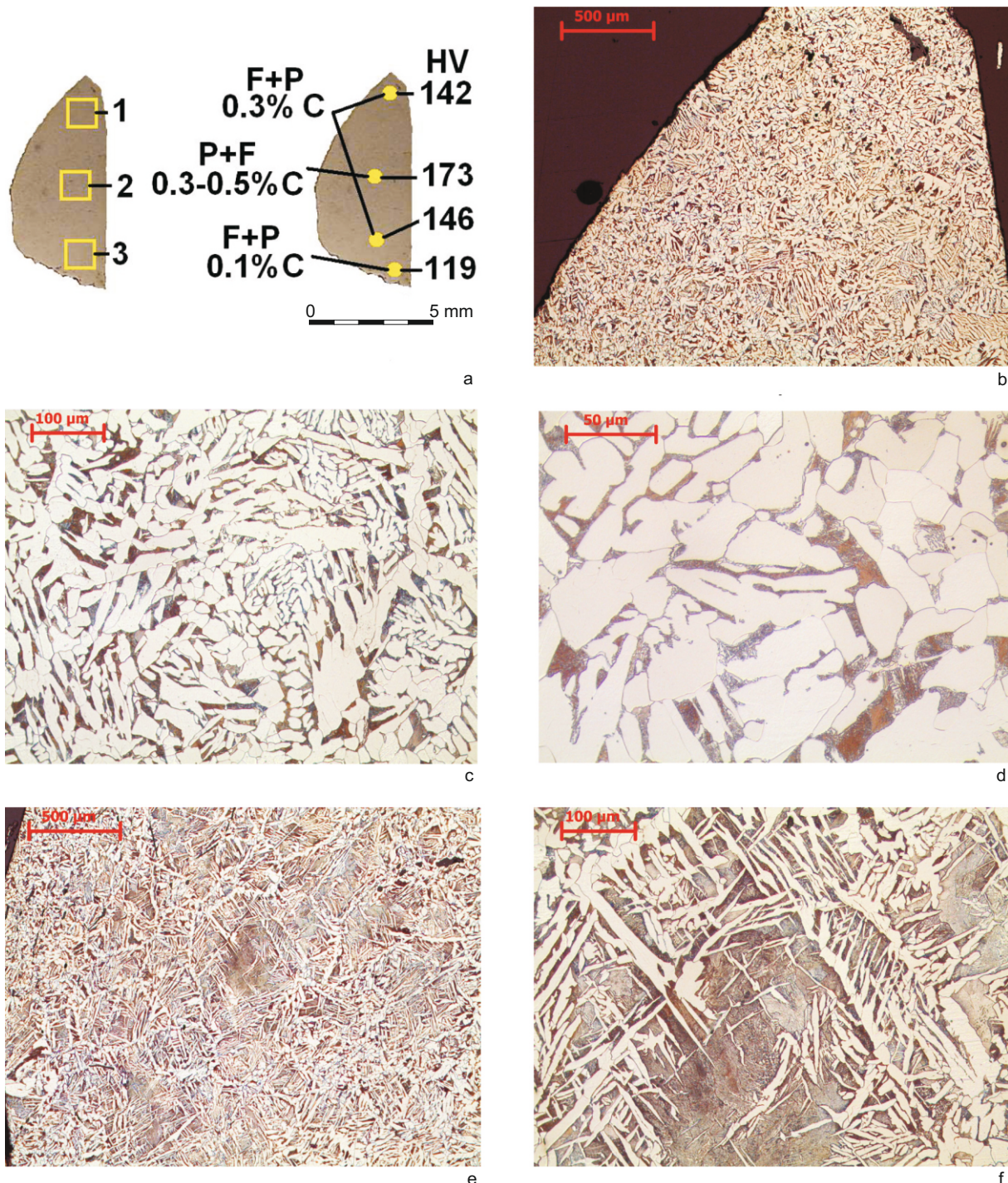


Fig. 6. Microstructures in the cross-section of the sample from the hackbut barrel, inv. No. MZM/421/MT: a – macrostructure of the sample with spots of microscopic observations (1-3); b – schematic depiction of distribution of structural components and results of HV10 hardness tests (F-ferrite, P-pearlite); c – ferritic-pearlitic microstructure in Spot 1; d-e – dark colonies of pearlite against the background of separations of bright granular ferrite and acicular Widmanstätten ferrite in Spot 1; f – pearlitic-ferritic microstructure in Spot 2; g – bright separations of acicular Widmanstätten ferrite against the background of dark pearlite in Spot 2.

Ryc. 6. Mikrostruktury na przekroju próbki z lufy hakownicy, nr inw. MZM/421/MT: a – makrostruktura próbki z miejscami obserwacji mikroskopowych (1-3); b – schematyczne przedstawienie rozmieszczenia składników strukturalnych i wyników testów twardości HV10 (F-ferryt, P-perlit); c – mikrostruktura ferrytyczno-perlityczna w miejscu 1; d-e – ciemne kolonie perlitu na tle wydzielen jasnego ziarnistego ferrytu i iglastego ferrytu Widmanstättena w miejscu 1; f – mikrostruktura perlityczno-ferrytyczna w miejscu 2; g – jasne wydzielenia iglastego ferrytu Widmanstättena na tle ciemnego perlitu w miejscu 2.

of the barrel are similar. The same can be said about the position of the touch hole (in this case, the priming pan survived). On the other hand,

the hook is much smaller (Konieczny 1964, 189, Pl. VIII) and it seems that its sole function was to mount the barrel in its wooden stock and not

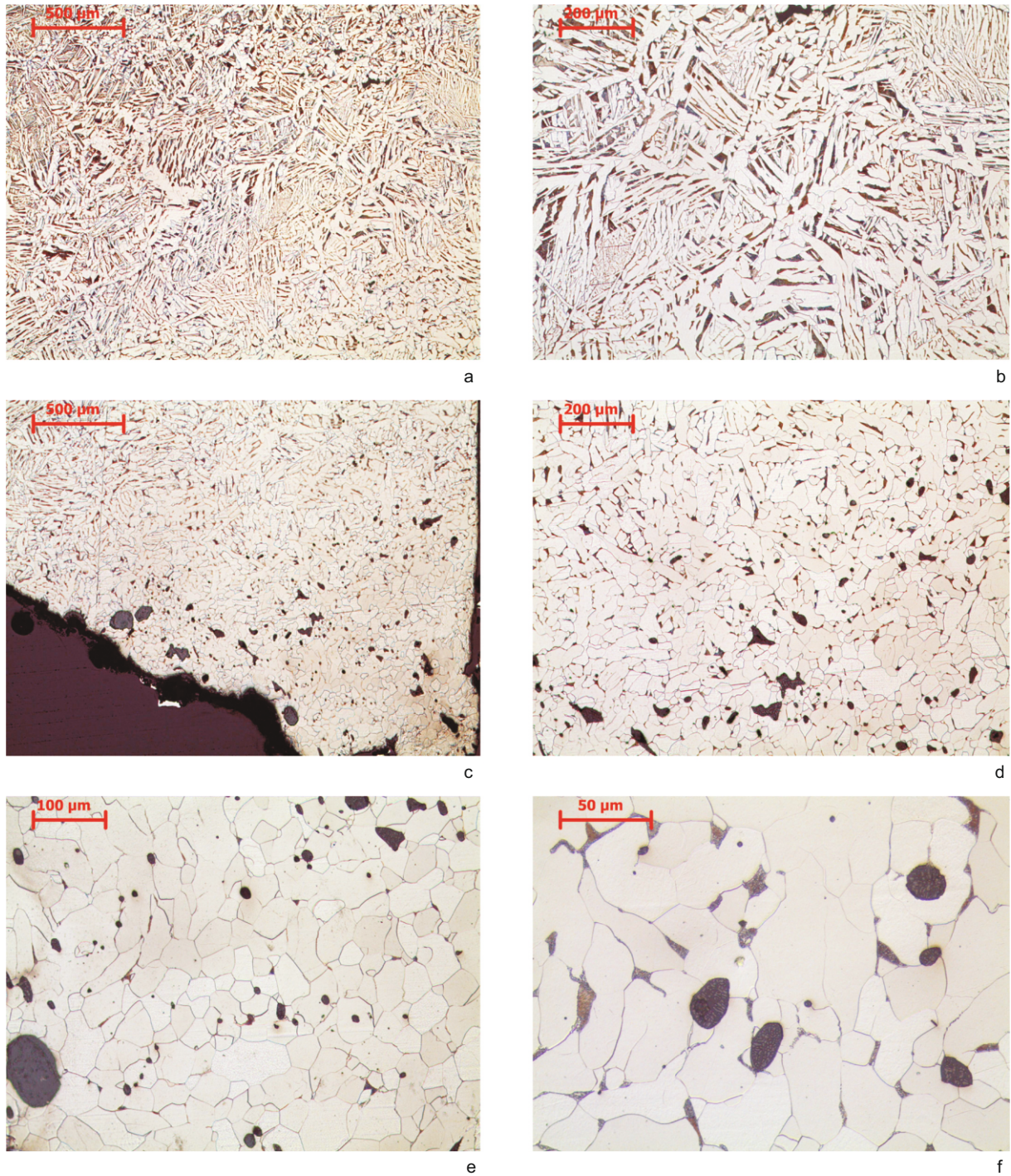


Fig. 7. Microstructures in the cross-section of the sample from the hackbut barrel, inv. No. MZM/421/MT: a-b – dark colonies of pearlite between acicular separations of Widmanstätten ferrite in Spot 2; c-d – ferritic-pearlitic microstructure and very numerous slag inclusions in Spot 3; e-f – sparse colonies of pearlite against the background of separations of granular ferrite and numerous globular slag inclusions in Spot 3.

Ryc. 7. Mikrostruktury na przekroju próbki z lufy hakownicy, nr inw. MZM/421/MT: a-b – ciemne kolonie perlitu między iglastymi wydzieleniami ferrytu Widmanstättena w miejscu 2; c-d – mikrostruktura ferrytyczno-perlityczna i bardzo liczne wtrącenia żużla w miejscu 3; e-f – nieliczne kolonie perlitu na tle wydzieleni ziarnistego ferrytu i licznych okrągłych wtrąceń żużla w miejscu 3.

to absorb the recoil when the gun was fired. Generally, this gun could rather be classified as a handgonne than hackbut in the strict sense of this term. More or less the same can be said

with regard to the other artefact (inv. No. MWP 299, early 16<sup>th</sup> century) (*ibid.*, 190, Pl. IX).

With regard to better analogies, B. Engel mentions a find of a heavy iron-forged hackbut,

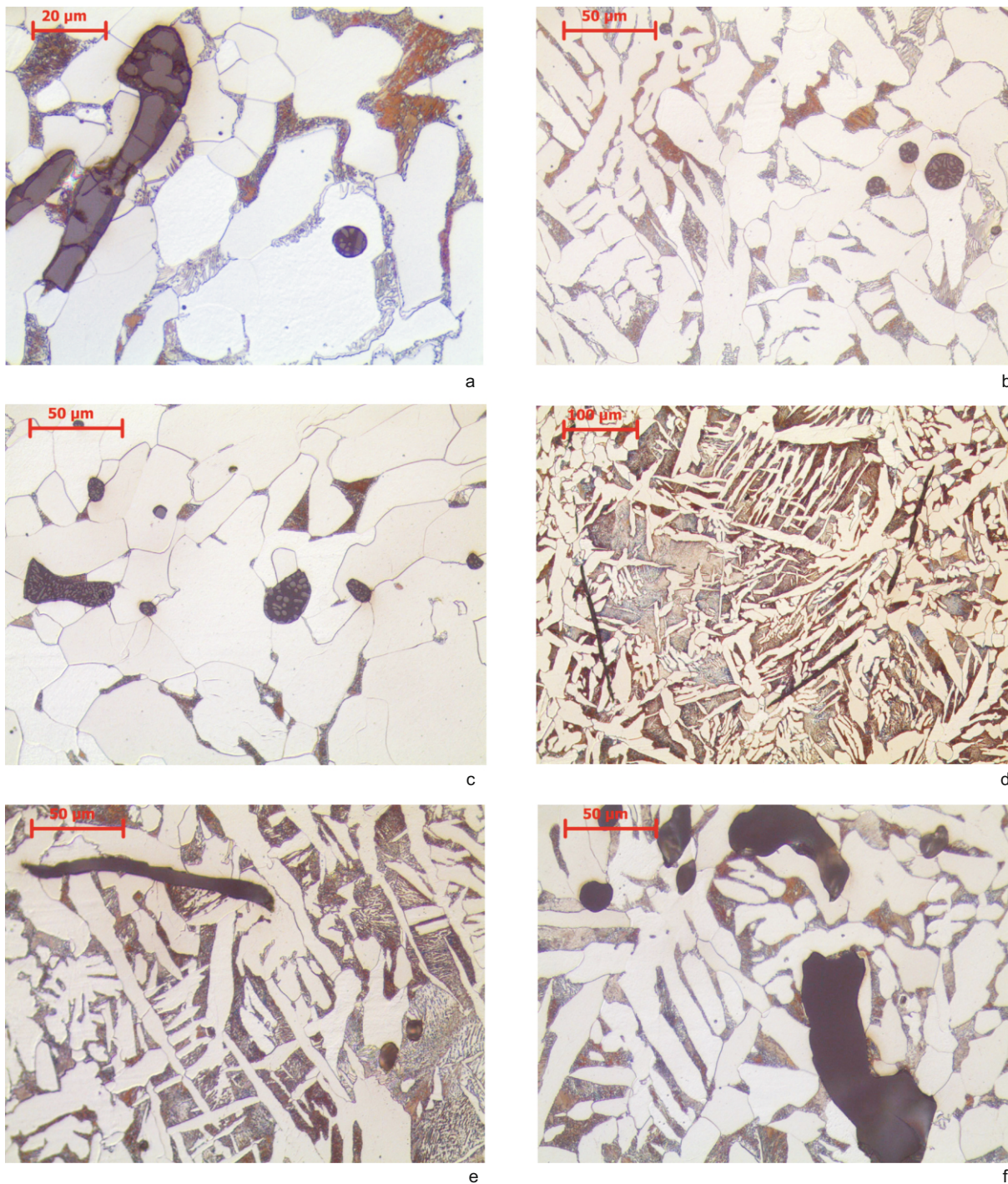


Fig. 8. Morphology of slag inclusions in the cross-section of the sample from the hackbut barrel, inv. No. MZM/421/MT: a-c – multi-phase slag inclusions, varying with regard to size and shape; d-f – single-phase slag inclusions, varying with regard to size and shape.

Ryc. 8. Morfologia wtrąceń żużla na przekroju próbki z lufy hakownicy, nr inv. MZM/421/MT: a-c – wielofazowe wtrącenia żużla różnej wielkości i kształtu; d-f – jednofazowe wtrącenia żużla różnej wielkości i kształtu.

discovered probably near Neuss in Rhineland and thus possibly related to the siege of this town by Duke Charles the Bold of Burgundy in 1474. Its dimensions and weight are quite similar to the discussed weapon (total weight 1070 mm, total weight ca. 12.5 kg, calibre 34 mm). However,

the hook is much shorter and its position is much more central. Furthermore, at the end of the barrel there is a socket with remains of an oak wood (?) shaft. On the other hand, the position of the touch hole, which is located on the right side of the breech, is analogous to the hackbut

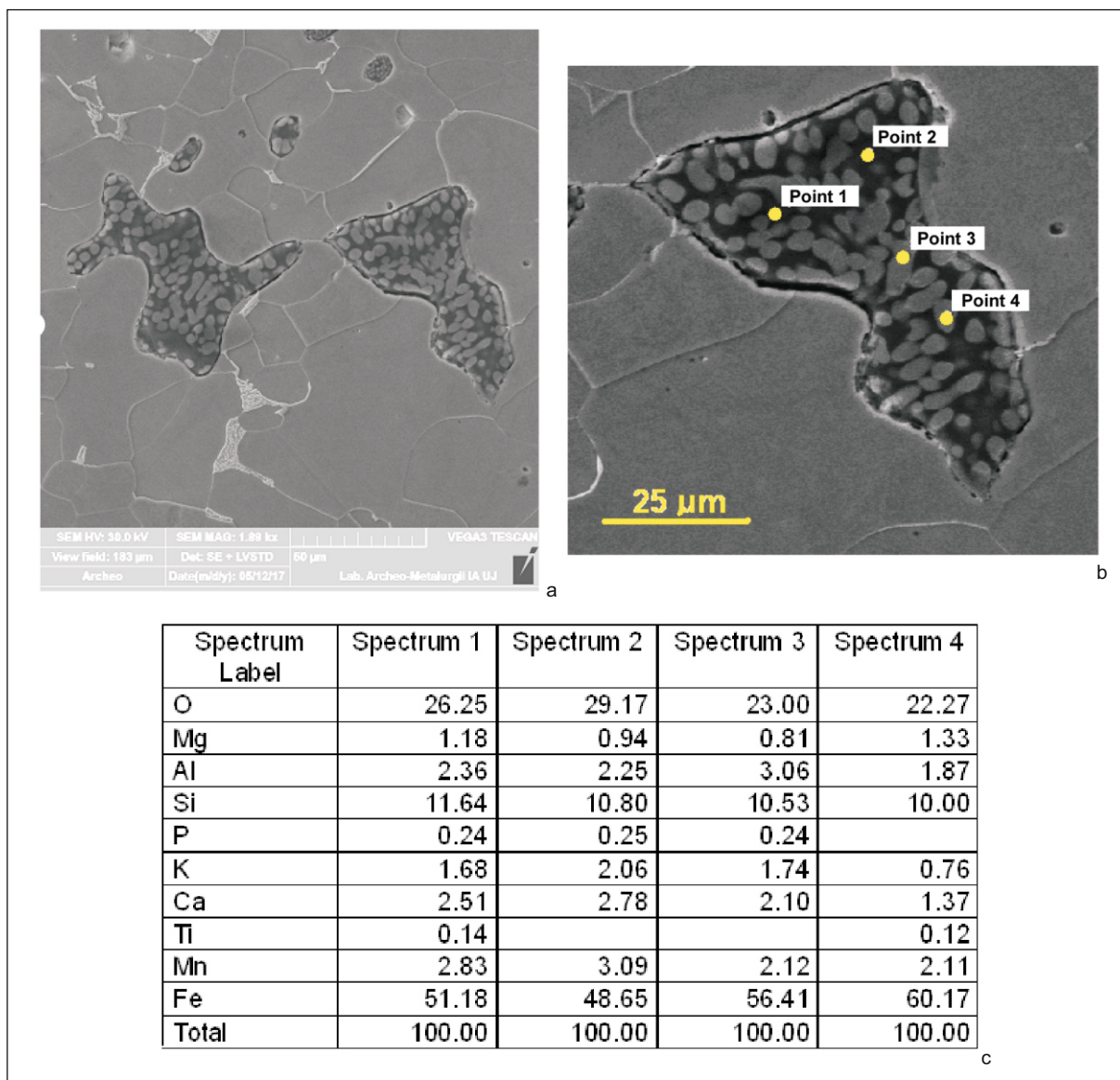


Fig. 9. Multi-phase slag inclusion (SII) in the cross-section of the sample from the hackbut barrel, inv. No. MZM/421/MT and its EDS point analysis: a – morphology of the multi-phase slag inclusion; b – analysed slag inclusion (SII): Points 1 and 2 are in the dark background of the inclusions, while Points 3 and 4 are in globular particles of the bright phase; c – results of quantitative EDS analysis in Points 1-4.

Ryc. 9. Wielofazowe wtrącenie żużla (SII) na przekroju próbki z lufy hakownicy, nr inw. MZM/421/MT i jego punktowa analiza EDS: a – morfologia wielofazowego wtrącenia żużla; b – analizowane wtrącenie żużla (SII): punkty 1 i 2 na ciemnym tle wtrącenia, punkty 3 i 4 na okrągłych cząsteczkach jasnej fazy; c – wyniki ilościowej analizy EDS w punktach 1-4.

from the Castle Museum. Another similarity is a possible presence of the foresight at the muzzle – what remains is a hole where the foresight may have been fixed. Additionally, there is a rearsight in the shape of a notch in a ring at the end of the breech (Engel 1900-1902, 302, Figs. 3-6).

Attention is also drawn to a fragment of an iron hackbut barrel discovered in 2003 at Helfštýn Castle in Bohemia (Fig. 3). The find was classified as a heavy siege hackbut (sometimes called “Doppelhacken”). Such weapons came

into existence ca. 1450 and remained in use to the mid-17<sup>th</sup> century. In this particular case, the hackbut could be dated to the turn of the 15<sup>th</sup> and 16<sup>th</sup> centuries, although it is tempting to relate the find to the siege of the castle by Matthias Corvinus King of Hungary (in 1468). On the other hand, a later chronology cannot be excluded, either. This is based on mentions of numerous hackbuts (including a burst one) in an inventory of the castle from 1552. This weapon displays several similarities to the hackbut from the Castle Museum. The barrel broadens near the muzzle

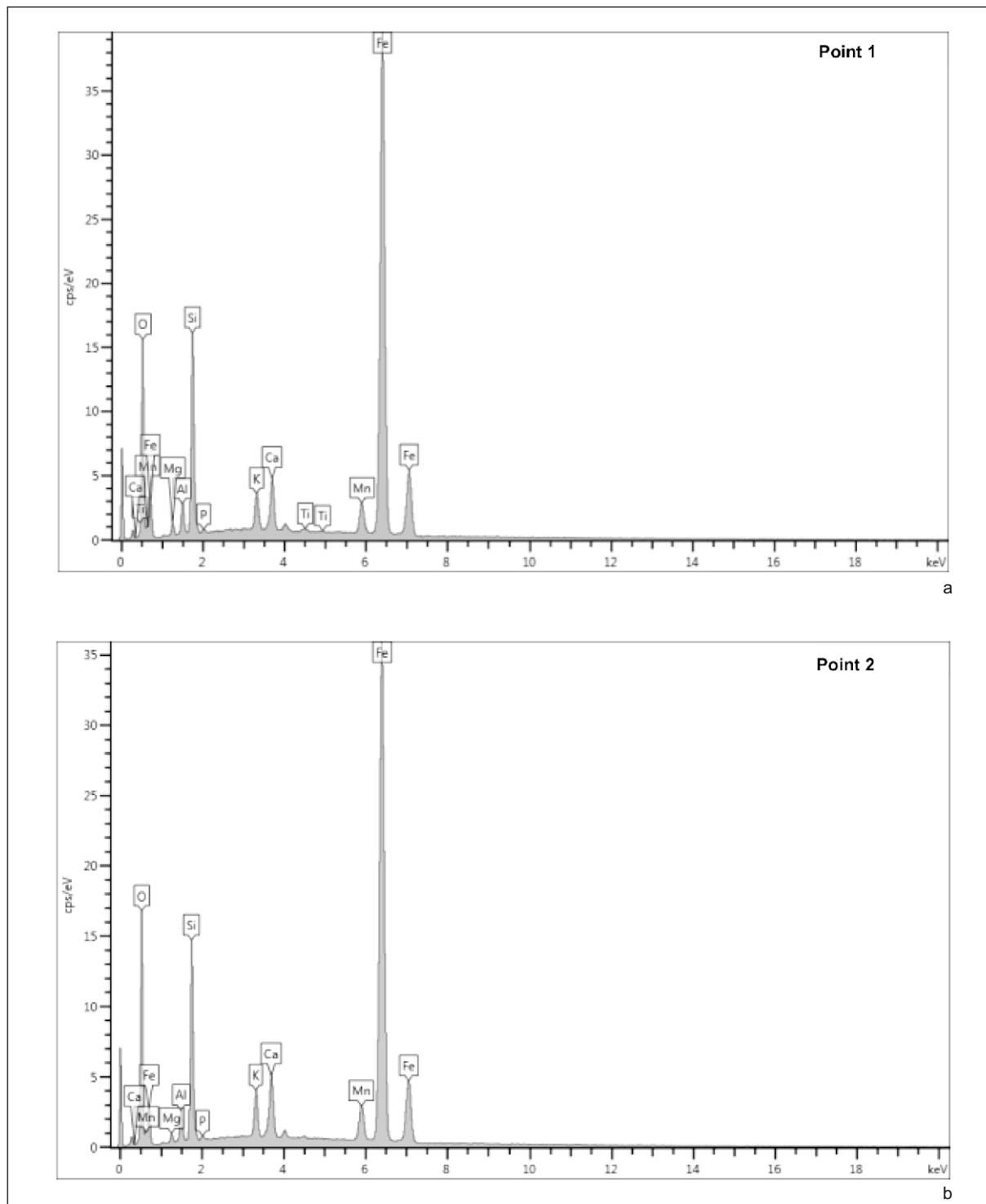


Fig. 10. EDS spectrums from the analysis of the dark background of the multi-phase slag inclusion (SI1): a – EDS analysis spectrum in Point 1; b – EDS analysis spectrum in Point 2.

Ryc. 10. Spektre EDS z analizy ciemnego tła wielofazowego wtrącenia żużla (SI1): a – spektrum analizy EDS w punkcie 1; b – spektrum analizy EDS w punkcie 2.

and narrows in the central part. Furthermore, it is also provided with a massive hook with an opening in the base. The location of the hook is analogous, too (Figel' et al. 2010, 476-481, Figs. 2, 3a; see also Strzyż 2014, cat. No. 75).

As it can be seen in Fig. 3, the thickness of the Helfštýn hackbut's walls is not even, which strongly suggests a construction analogy to the Castle Museum barrel. It is of interest that the spot of bursting of the Helfštýn gun

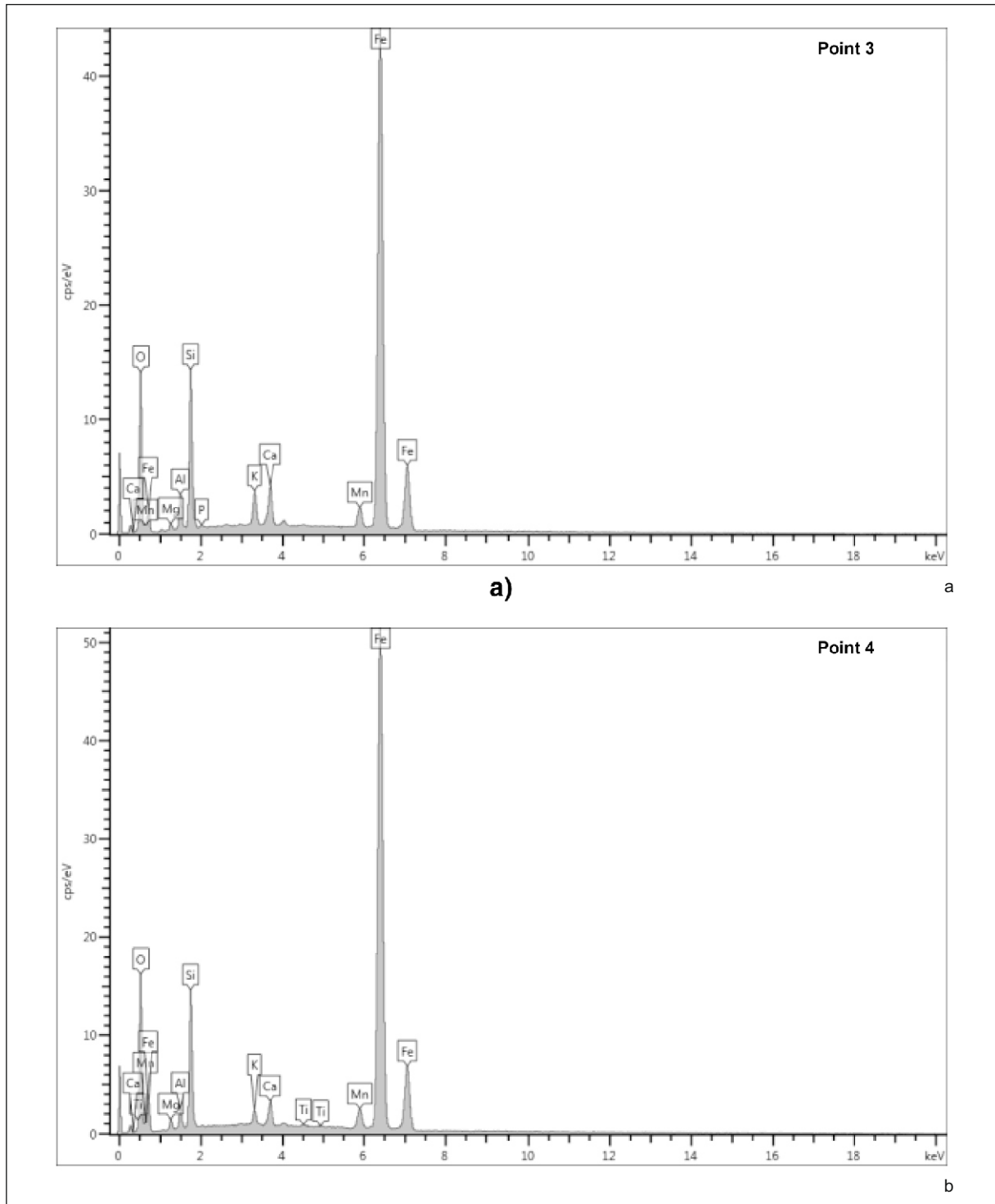


Fig. 11. EDS spectrums from the analysis of bright globular separations in the multi-phase slag inclusion (SI1): a – EDS analysis spectrum in Point 3; b – EDS analysis spectrum in Point 4.

Ryc. 11. Spektre EDS z analizy jasnych okrągłych wydzielen w wielofazowym wtrąceniu żużla (SI1): a – spektrum analizy EDS w punkcie 3; b – spektrum analizy EDS w punkcie 4.

is located near the hook. As said above, it is precisely in this place that the walls of the Castle Museum hackbut were in all probability the thinnest (see Fig. 1:1). Therefore, the same trait could also be supposed here. It is

remarkable that technological examinations of the Helfštýn hackbut also revealed manufacturing imperfections (a too high content of phosphorus in the metal and a too high temperature of forging, see below).

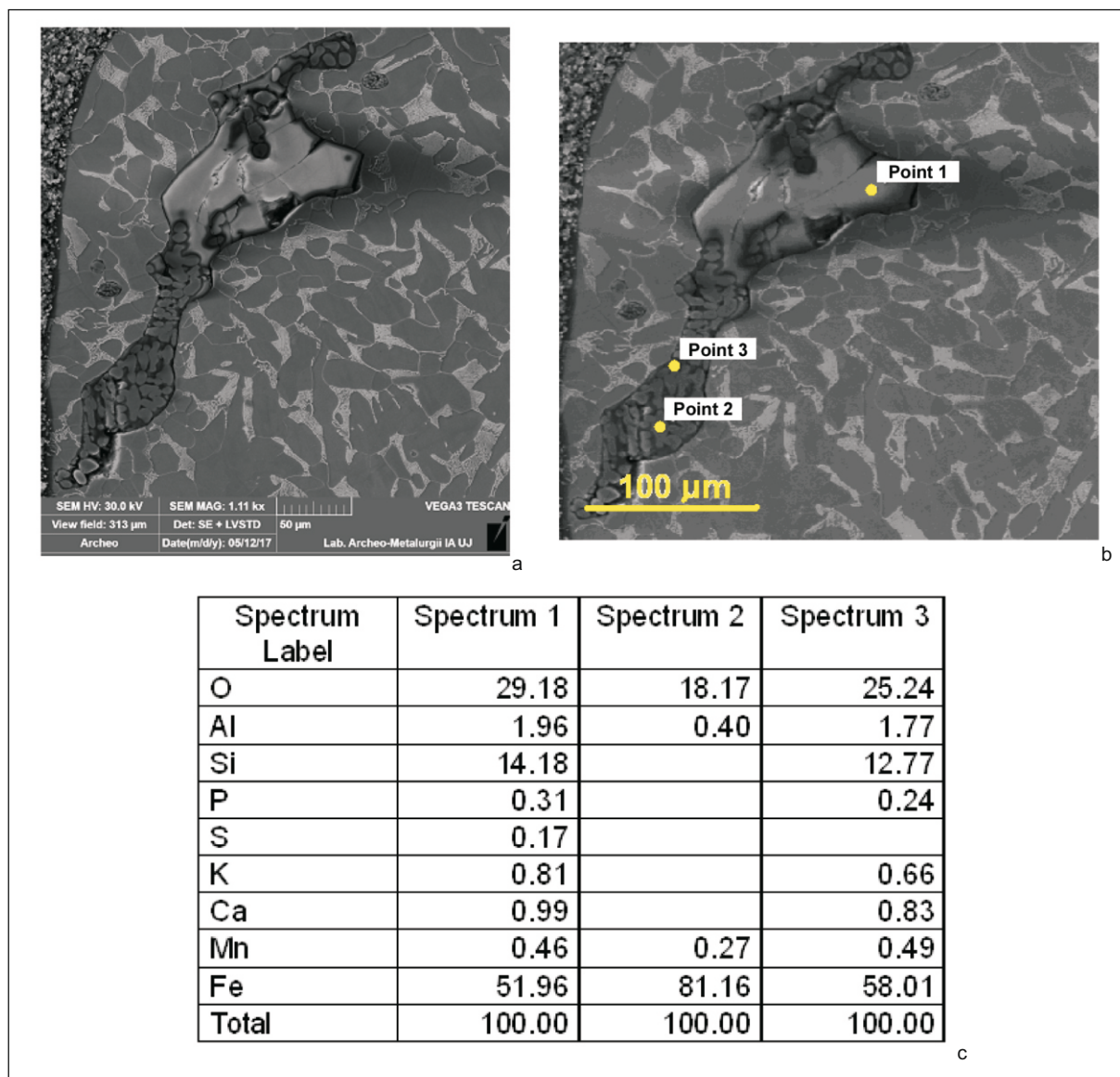


Fig. 12. Multi-phase slag inclusion (SI2) in the cross-section of the sample from the hackbut barrel, inv. No. MZM/421/MT and their EDS point analysis: a – morphology of the multi-phase slag inclusion; b – analysed points in the slag inclusion: Point 1 (bright solid background), Point 2 (dark background), Point 3 (bright globular particles); c – results of the quantitative EDS analysis in Points 1-3.

Ryc. 12. Wielofazowe wtrącenie żużla (SI2) na przekroju próbki z lufy hakownicy, nr inw. MZM/421/MT i jego punktowa analiza EDS: a – morfologia wielofazowego wtrącenia żużla; b – analizowane punkty na wtrąceniu żużla: punkt 1 (jasne tło), punkt 2 (ciemne tło), punkt 3 (jasne okrągłe cząsteczki); c – wyniki analizy ilościowej EDS w punktach 1-3.

Moreover, D. Figel', M. Hložek, J. Hošek, Z. Schenk and P. Žákovský mention numerous analogies to the Helfštýn weapon. With regard to the Castle Museum hackbut, the most significant ones are two artefacts from the National Museum in Prague (Fig. 4). They are almost identical as the weapon which is discussed in the present paper, save the fact that they seem to be somewhat more slender. They also display numerous constructional analogies, such as tangs at the ends of their breeches, catches in their back parts, or very similar touch holes. Another similarity is

offered by massive hooks with openings in their bases (Figel' et al. 2010, 480, 482, Fig. 7).

Another important remark made by D. Figel', M. Hložek, J. Hošek, Z. Schenk and P. Žákovský concerns several depictions of such weapons in contemporary manuscript sources. The most relevant one is the well-known "Zeugbuch" of Maximilian I (ca. 1502) (ibid., 477, 479-481, Fig. 5 – on the other hand, this image depicts brass hackbuts). The "Zeugbuch" depicts a series of iron-forged hackbuts (*geschmidt hagkennbuchsen*) provided with massive butts. There are some

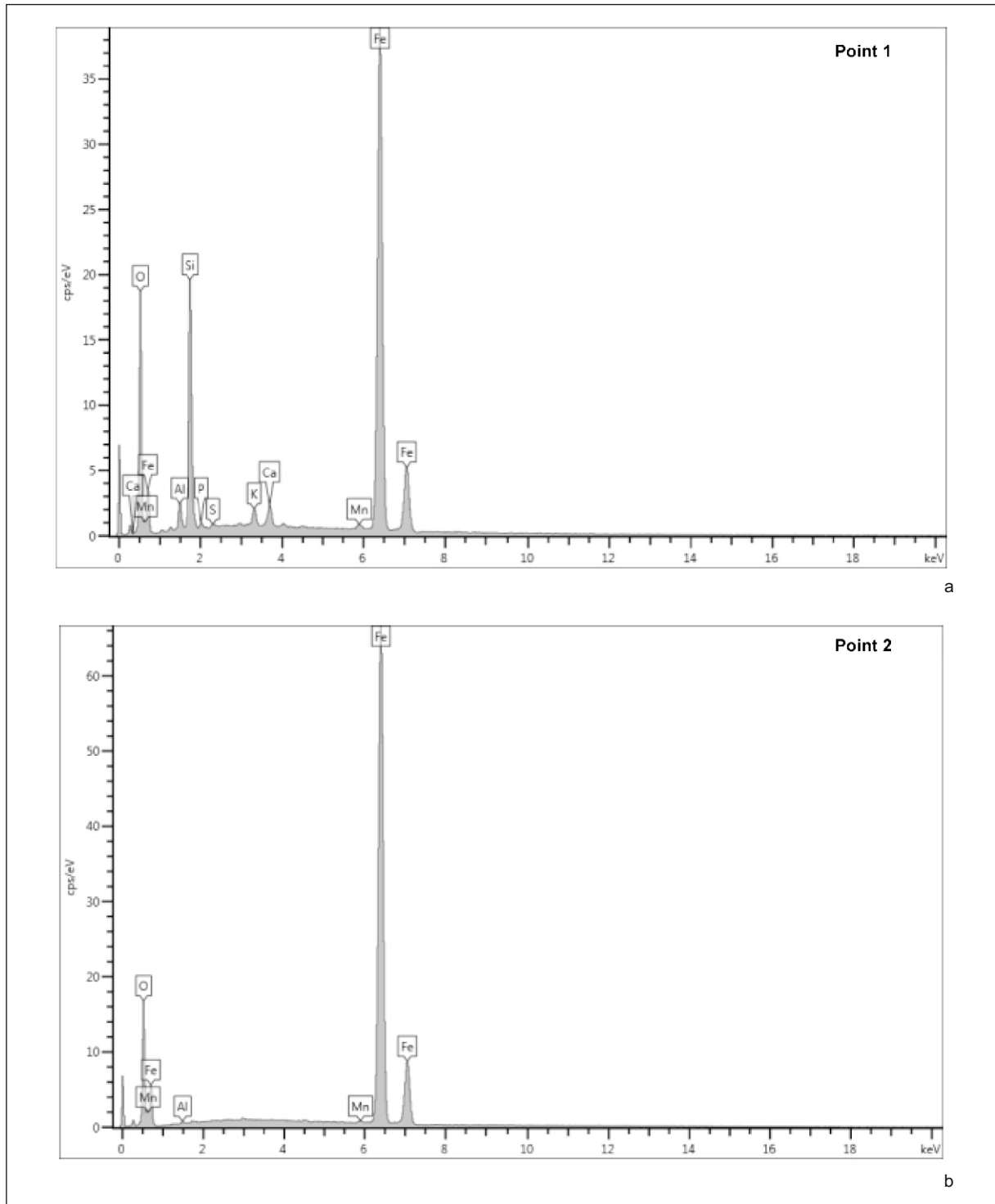


Fig. 13. EDS spectrums from the analysis of the multi-phase slag inclusion (SI2): a – EDS analysis spectrum in Point 1; b – EDS analysis spectrum in Point 2.

Ryc. 13. Spektre EDS z analizy wielofazowego wtrącenia żużla (SI2): a – spektrum analizy EDS w punkcie 1; b – spektrum analizy EDS w punkcie 2.

differences between these weapons and the discussed artefact. The shape of their hooks is different, as they are more chamfered in their lower parts. Furthermore, no catches can be seen in their breech parts (*Zeugbuch*, 73r). With regard to that,

the discussed weapon would perhaps be more similar to brass hackbuts from this manuscript (Fig. 5:1). In some of these, the butt extends into a long stock which runs under the barrel beyond the hook. It can be assumed that there is an opening

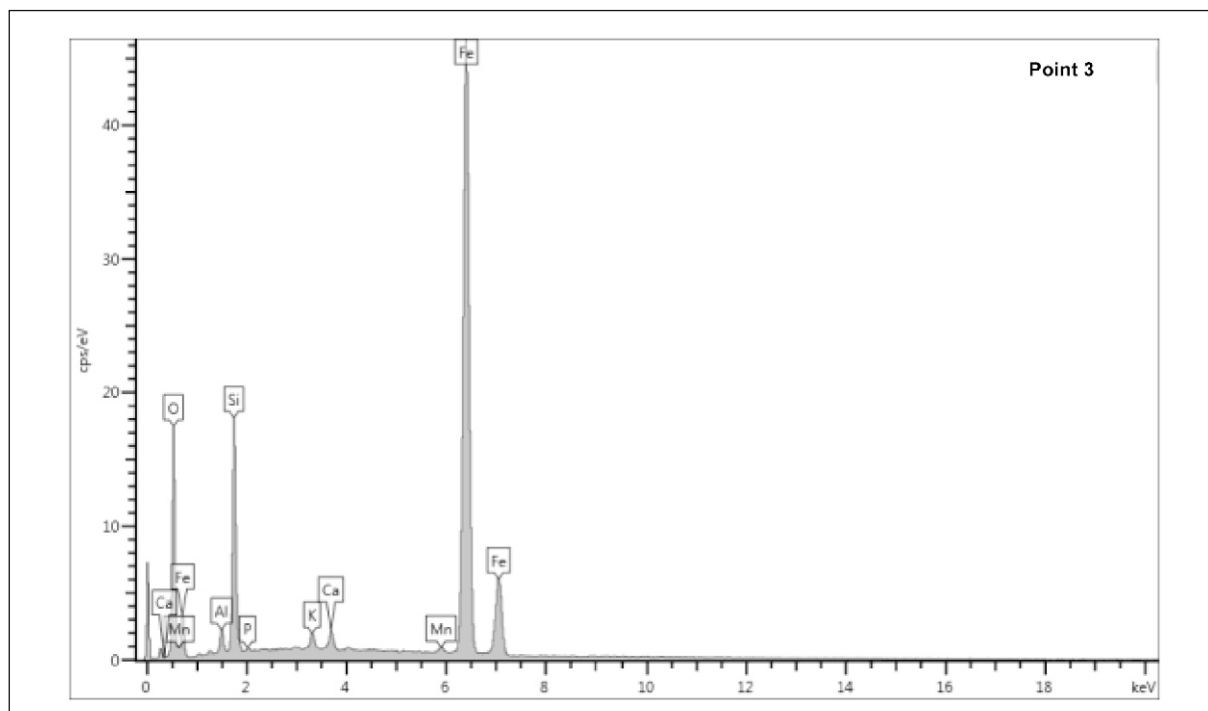


Fig. 14. EDS spectrum from the analysis of the dark background of the multi-phase slag inclusion (SI2). EDS analysis spectrum in Point 3.

Ryc. 14. Spektrum EDS z analizy ciemnego tła wielofazowego wtrącenia żużla (SI2). Spektrum analizy EDS w punkcie 3.

in the hook's base. This is implied by the presence of a peg which fastens the stock to the hook. Analogously, the presence of a catch in the breech part of the barrel is suggested by another peg in the stock. Furthermore, priming pans can be seen on the right side of the breeches (*Zeugbuch*, ca. 72v).

Furthermore, the "Zeugbuch" also provides information on the use of such hackbuts (Fig. 5:2). The weapon is operated by a team of two landsknechts. It is supported with its hook on a wooden iron-fitted trestle and it is fired with a hand-held slow match (*Zeugbuch*, 72r, 73r; for large hackbuts and two-person firing teams operating such weapons see also Forrer 1905, 28, Fig. 6:a; Głosek 1990, 158; Szymczak 2004, 41-45, 59; Strzyż 2014, 57-59).

An interesting hackbut was discussed by R. Forrer. It was part of his private collection of firearms and was of possibly Austrian provenance. This can be assumed on the basis of an inspection mark of the city of Vienna. The weapon was found in the moat of the town of Nieheim in Westphalia. The proposed chronology of the hackbut is ca. 1490-1500. Its breech part is burst by an explosion. It is an iron-forged gun with a total length of 94.5 cm, a total weight of 9 kg and a calibre of 2.75-3 cm. Its octagonal barrel is provided both with a foresight and a rearsight.

A massive chamfered hook with an opening in its base is located in the central part of the barrel. There are also two catches with openings, placed in the front and rear part of the barrel. R. Forrer had its stock reconstructed and had a new trestle made (Forrer 1905, 29, Fig. 7). The trestle seems to imitate those from the afore-mentioned images in the "Zeugbuch".

Another interesting analogy is a heavy iron-forged hackbut from Ustyuzha-Zelezopolskaya in Russia, now in the collection of the Military-Historical Museum of Artillery, Engineer and Signal Corps in St Petersburg (Inv. No. 10/313). It is dated to the mid-16<sup>th</sup> century. Analogously to the Castle Museum weapon, this gun is also provided with a massive (albeit more slender) hook with an opening and a catch can be seen under the breech. In the rear part of the barrel there is a rearsight. In contrast to the hackbut from the Castle Museum, the Russian gun does not narrow in its central part, but it seems to slightly taper from the hook toward the muzzle (Маковская 1992, 56-57, 161, Fig. 96).

Several interesting examples of iron hackbuts (although none of these can be seen as an exact analogy to the discussed barrel) are mentioned in the work of P. Strzyż. One of these comes from the ruins of the castle in Buda in Hungary and it is dated to the period between the late 15<sup>th</sup> century

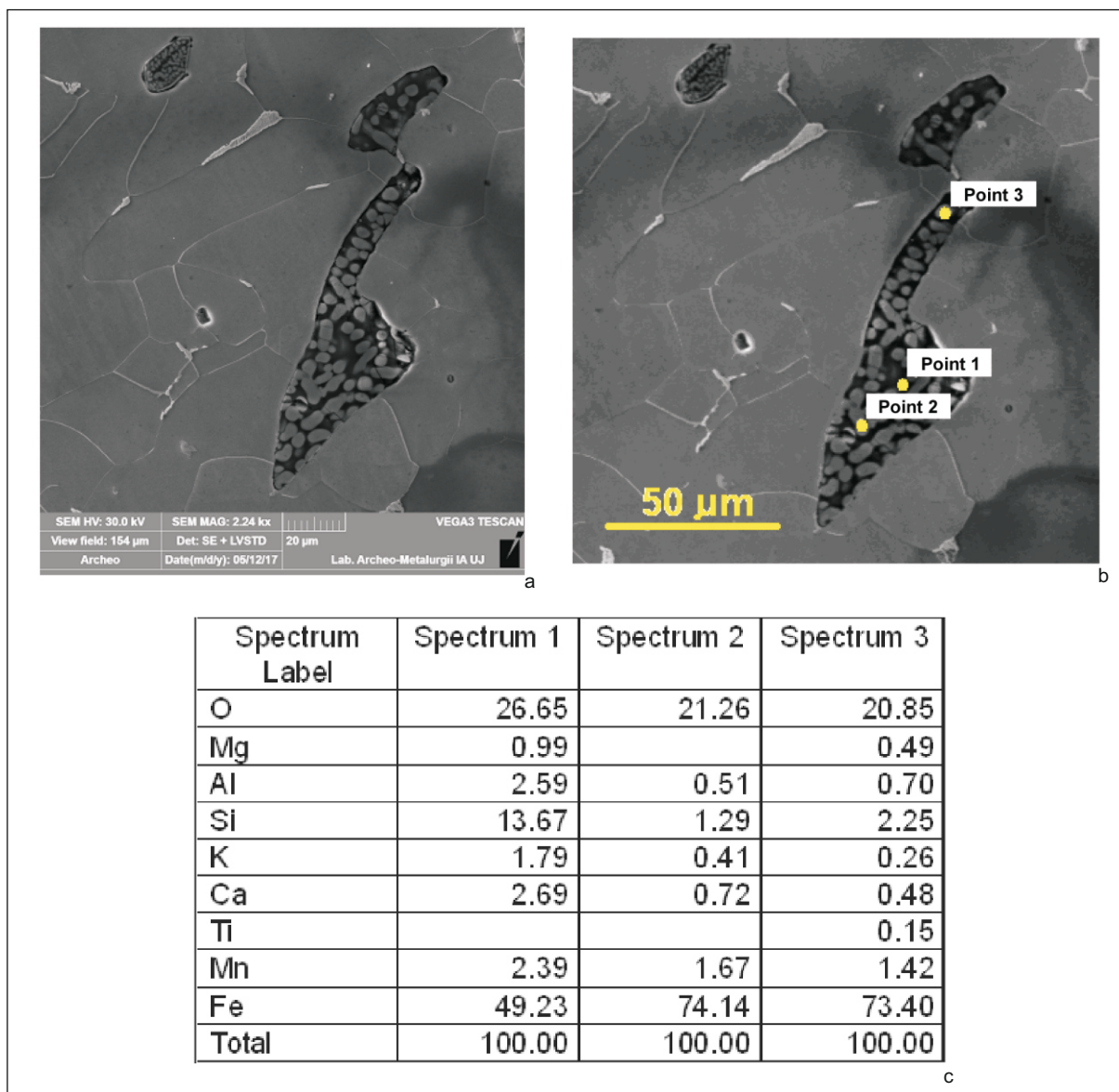


Fig. 15. Multi-phase slag inclusion (SI3) in the cross-section of the sample from the hackbut barrel, inv. No. MZM/421/MT and its EDS point analysis: a – morphology of the multi-phase slag inclusion; b – analysed points in the slag inclusion: Point 1 (dark background), Points 2 and 3 (bright globular particles); c – results of the quantitative EDS analysis in Points 1-3.

Ryc. 15. Wielofazowe wtrącenie żużla (SI3) na przekroju próbki z lufy hakownicy, nr inw. MZM/421/MT i jego punktowa analiza EDS: a – morfologia wielofazowego wtrącenia żużla; b – analizowane punkty na wtrąceniu żużla: punkt 1 (ciemne tło), punkty 2 i 3 (jasne okrągłe cząsteczki); c – wyniki analizy ilościowej EDS w punktach 1-3.

and about 1525. Its total length is 119 cm and its calibre is 2.2 cm. In the front part of the barrel there is a massive chamfered hook. The touch hole and a feebly pronounced priming pan are located on the right side of the barrel. A long and slightly bent tang extends from the breech part (Strzyż 2014, 339, Pl. LIX:1-4, Cat. No. 141).

An interesting find of a heavy iron-forged hackbut was discovered in the battlefield in Mohács in Hungary, where a battle was fought

in 1526 between Hungarian and Turkish forces. The weapon is dated to the late 15<sup>th</sup> century – about 1525. Its total length is 89 cm and its calibre is 2.4 cm. The weight of the gun is 11.2 kg. In the front part of the barrel there is a massive chamfered hook with an opening in its central part. In the rear part of the gun there is a short and slightly bent massive tang, also provided with an opening. The touch hole is located in the right side of the barrel (ibid., 340, Pl. LX:1-3, Cat.No. 156).

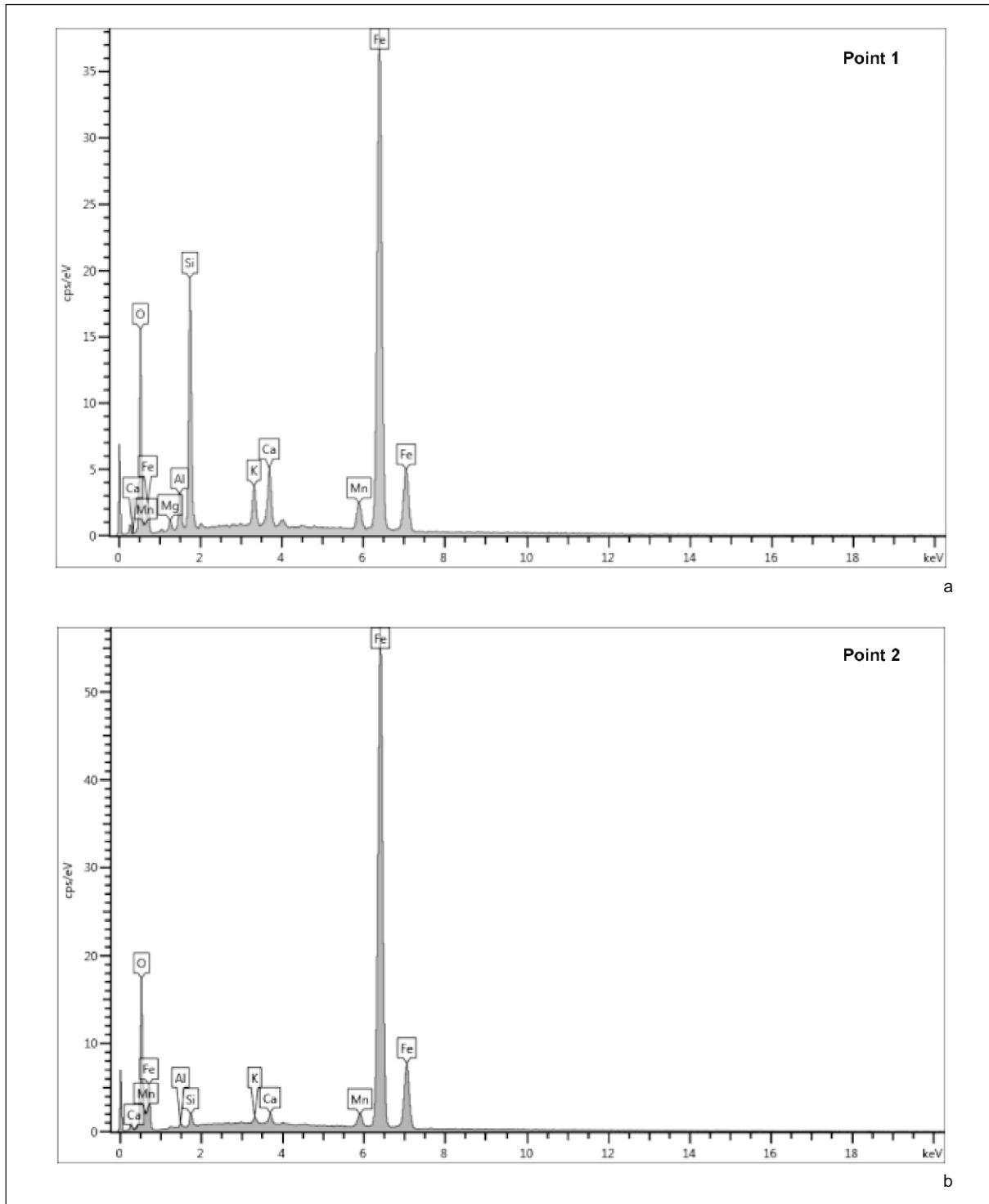


Fig. 16. EDS spectrums from the analysis of the multi-phase slag inclusion (SI3): a – EDS analysis spectrum in Point 1 (dark background); b – EDS analysis spectrum in Point 2 (bright globular particle).

Ryc. 16. Spekttra EDS z analizy wielofazowego wtrącenia żużła (SI3): a – spektrum analizy EDS w punkcie 1 (ciemne tło); b – spektrum analizy EDS w punkcie 2 (jasne okrągłe cząsteczki).

Yet another interesting iron hackbut (of unknown provenance) is kept in the collection of the Hungarian National Museum in Budapest. Its total length is 153.5 cm, its calibre is 2.5 cm

and its weight is 12.5 kg. The weapon is dated to the end of the 15<sup>th</sup> – the first quarter of the 16<sup>th</sup> century. A massive chamfered hook can be seen in the front part of the barrel. The weapon

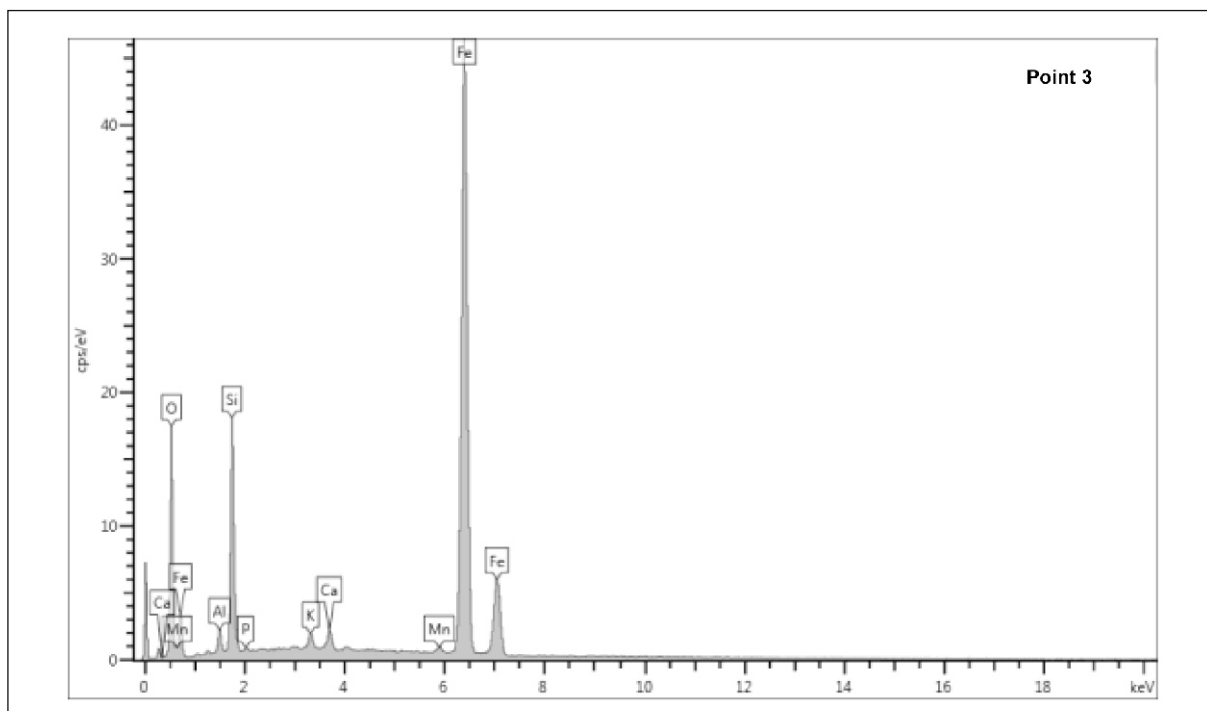


Fig. 17. EDS spectrum from the analysis of the multi-phase slag inclusion (SI3). EDS analysis spectrum in Point 3 (bright globular particle).

Ryc. 17. Spektum EDS z analizy wielofazowego wtrącenia żużla (SI3). Spektum analizy EDS w punkcie 3 (jasna okrągła cząsteczka).

is provided both with a foresight and a rearsight. The touch hole is located on the right side of the barrel. The weapon ends with a long and slightly bent tang, provided with a look at its end (*ibid.*, 338, Pl. LVIII:1-5, Cat. No. 169).

In the Hungarian National Museum in Budapest there is also another interesting heavy iron-forged hackbut. Its total length is 103 cm, its calibre is 2.1 cm and its weight is 15 kg. The weapon's chronology falls between the late 15<sup>th</sup> and the first quarter of the 16<sup>th</sup> century. Apart from a massive chamfered hook with an opening, the barrel is also provided with two catches in its rear part. On the right side of the breech there is a massive priming pan with a touch hole. The barrel is provided both with a rearsight and a foresight (*ibid.*, 337, Pl. LVII:1-7, Cat. No. 171).

Another iron-forged hackbut is known from Győr in Hungary. This weapon is dated to ca. 1450-1525. Its total length is 102.2 cm and its calibre is 2.3 cm. The barrel is also provided with a massive chamfered hook in its front part. The touch hole is located on the right side of the barrel and there is a long and slender tang in the rear part of the gun. Interestingly, there are circumferential grooves in the breech part (*ibid.*, 344, Pl. LXIV:1-4, Cat. No. 147).

In the light of the aforementioned examples,<sup>2</sup> the artefact in question can be classified as a heavy siege hackbut, which was in all probability operated using a wooden trestle, as depicted in the “Zeugbuch”. The chronology of the gun, bearing in mind a complete lack of contextual data, can be defined only in a very approximate manner. The hackbut may have been made in the late 15<sup>th</sup> or early 16<sup>th</sup> century. However, it may have remained in use long after that time, even to the mid-17<sup>th</sup> century (on later use of such hackbuts see also *ibid.*, 63).

#### Archaeometallurgical examinations of the barrel

A wedge-shaped sample was taken from the internal side of the muzzle. The sample was mounted in epoxy resin and then it was ground and polished with the use of diamond pastes of various grits. The polished surface of the sample was etched with 4% nital in order to reveal its microstructure. Microstructure observations were done with the use of a Leica DMLM optical microscope. The analysis of slag inclusions was carried out with the use of a Tescan Vega Super 3 scanning microscope, equipped with an EDS type spectrometer. Observations were conducted using 30 kV accelerating voltage. The content of carbon in

<sup>2</sup> For other possible analogies see, e.g., Kalmár (1971, 194, Fig. 114; see also Šnajdrová 1998).

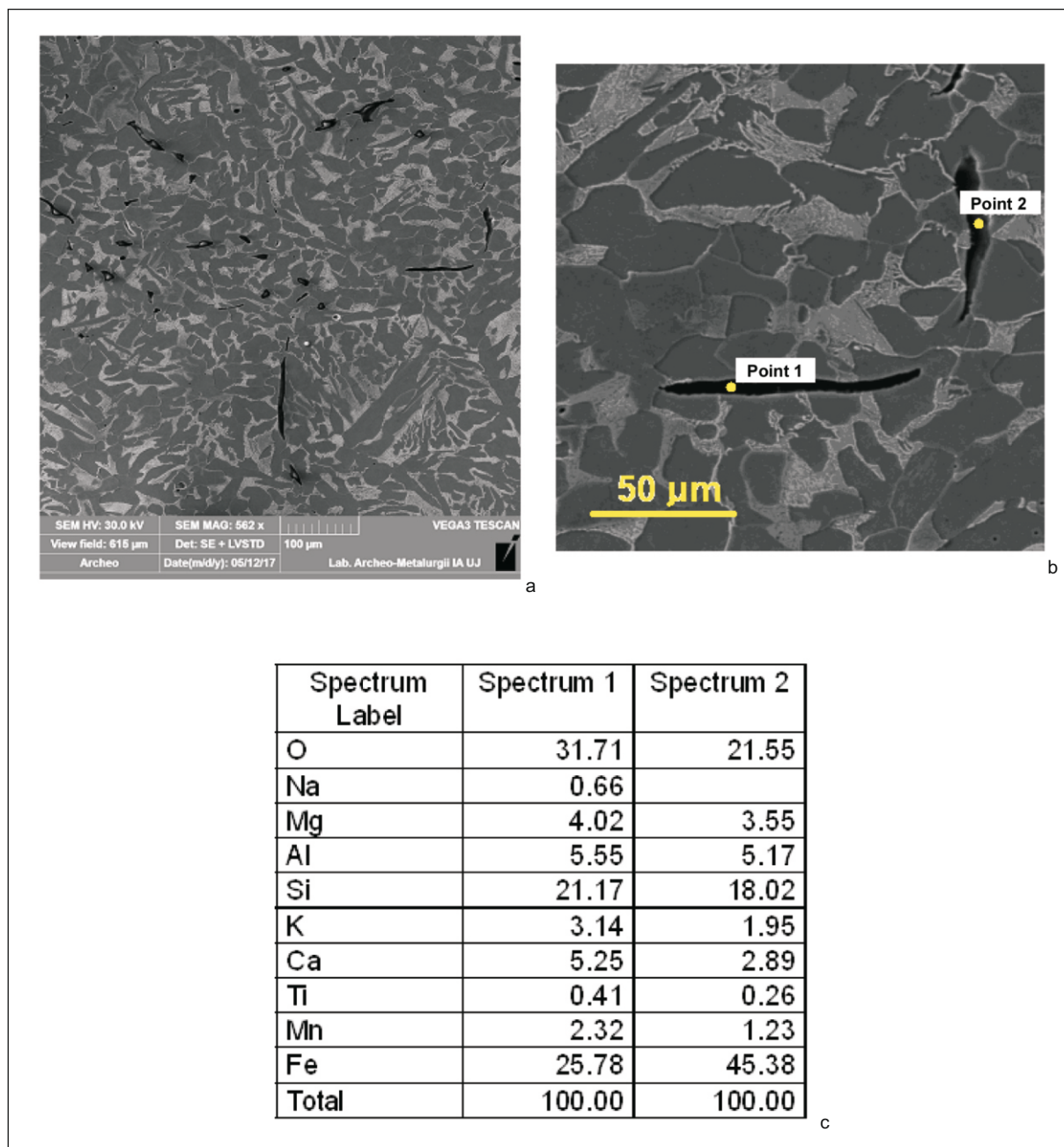


Fig. 18. Single-phase slag inclusions (SI4) in the cross-section of the sample from the hackbut barrel, inv. No. MZM/421/MT and their EDS point analysis: a – morphology of single-phase slag inclusions; b – analysed slag inclusions, Points 1 and 2 (dark background); c – results of EDS quantitative analysis in Points 1 and 2.

Ryc. 18. Jednofazowe wtrącenia żużla (SI4) na przekroju próbki z lufy hakownicy, nr inw. MZM/421/MT i ich punktowa analiza EDS: a – morfologia jednofazowych wtrąceń żużla; b – analizowane wtrącenia żużla, punkty 1 i 2 (ciemne tło); c – wyniki analizy ilościowej EDS w punktach 1 i 2.

the sample was assessed on the basis of microscopic observations. Hardness tests were done using the Vickers method with a load of 10kG (98N).

#### Microscopic examinations and the EDS analysis of slag inclusions

A macroscopic image of the sample's surface with spots of microscopic observations (1-3) and

a schematic distribution of structural components and results of HV10 hardness tests can be seen in Fig. 6:a-b.

Microscopic observations revealed the presence of ferritic-pearlitic microstructures in Spots 1 and 3 (Fig. 6:a). This corresponds to soft steel with the content of carbon of 0.2-0.3% C (Figs. 6:c-e and 7:c-d). Locally in Spot 3 the carbon

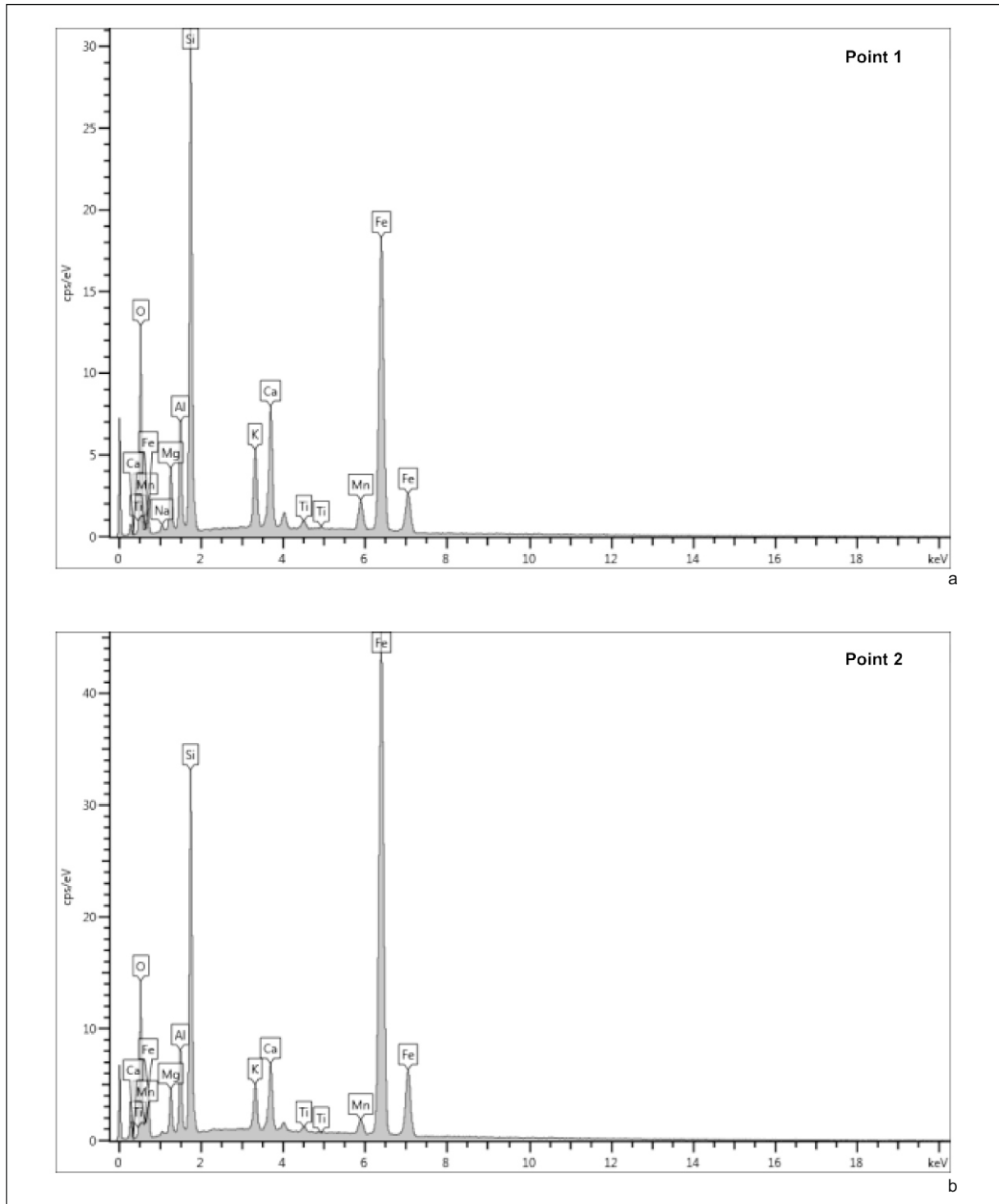
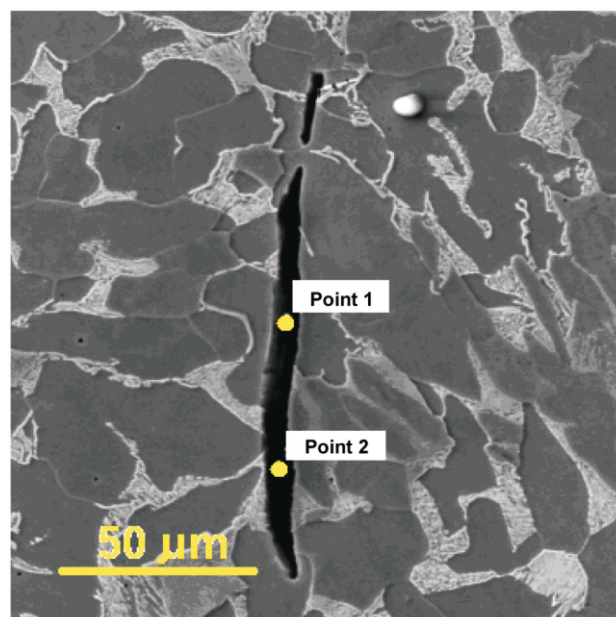


Fig. 19. EDS spectrums from the analysis of single-phase slag inclusions (SI4): a – EDS analysis spectrum in Point 1 (dark background); b – EDS analysis spectrum in Point 2 (dark background).

Ryc. 19. Spekttra EDS z analizy jednofazowych wtrąceń żużla (SI4): a – spektrum analizy EDS w punkcie 1 (ciemne tło); b – spektrum analizy EDS w punkcie 2 (ciemne tło).

content is even lower, i.e., 0.1% C (Fig. 7:e-f). In the remaining area of the sample (Spot 2) there is pearlitic-ferritic microstructure corresponding to semi-hard steel with the content of carbon of 0.3-0.5% C (Figs. 10:e-f and 11:a-b). A remarkable

trait of the microstructure is the presence of high amounts of acicular ferrite (so-called Widmanstätten structures, Figs. 6:b-f and 7:a-b). Such structures can be seen both inside grains and near borders of former austenite. These structures usually come



a

Spectrum Label	Spectrum 1	Spectrum 2
O	33.65	34.80
Na	0.53	0.55
Mg	4.00	4.02
Al	6.51	6.57
Si	24.57	24.56
K	4.03	4.09
Ca	6.55	6.72
Ti	0.54	0.50
Mn	1.93	1.93
Fe	17.68	16.26
Total	100.00	100.00

b

Fig. 20. Multi-phase slag inclusion (SI5) in the cross-section of the sample from the hackbut barrel, inv. No. MZM/421/MT and its EDS point analysis: a – morphology of the single-phase slag inclusion; b – analysed slag inclusion, Points 1 and 2 (dark background); c – results of EDS analysis in Points 1 and 2.

Ryc. 20. Wielofazowe wtrącenie żużla (SI5) na przekroju próbki z lufy hakownicy, nr inw. MZM/421/MT i jego punktowa analiza EDS: a – morfologia jednofazowego wtrącenia żużla; b – analizowane wtrącenie żużla, punkty 1 i 2 (ciemne tło); c – wyniki analizy ilościowej EDS w punktach 1 i 2.

into existence in result of accelerated cooling of overheated steel, that is, after the metal was improperly heated for forging.

Numerous slag inclusions (SI) can be seen in the metal. These are both single- (SI4, SI5, SI6) and multi-phase (SI1, SI2, SI3, SI7) and they locally form clusters. The morphology of these inclusions (seen under the optical microscope)

can be see in Fig. 8. The EDS X-ray microanalysis of multi-phase slag inclusions (SI1, SI2, SI3, SI7) demonstrates that bright globular particles chiefly contain Fe and O – these are separations of wüstite (Figs. 9-17 and 24-26). On the other hand, in the background of multi-phase slag inclusions there are such elements as Fe, Si, O, Ca, K, Mn, Al, Mg, P, S and Ti (Figs. 9, 12, 15,

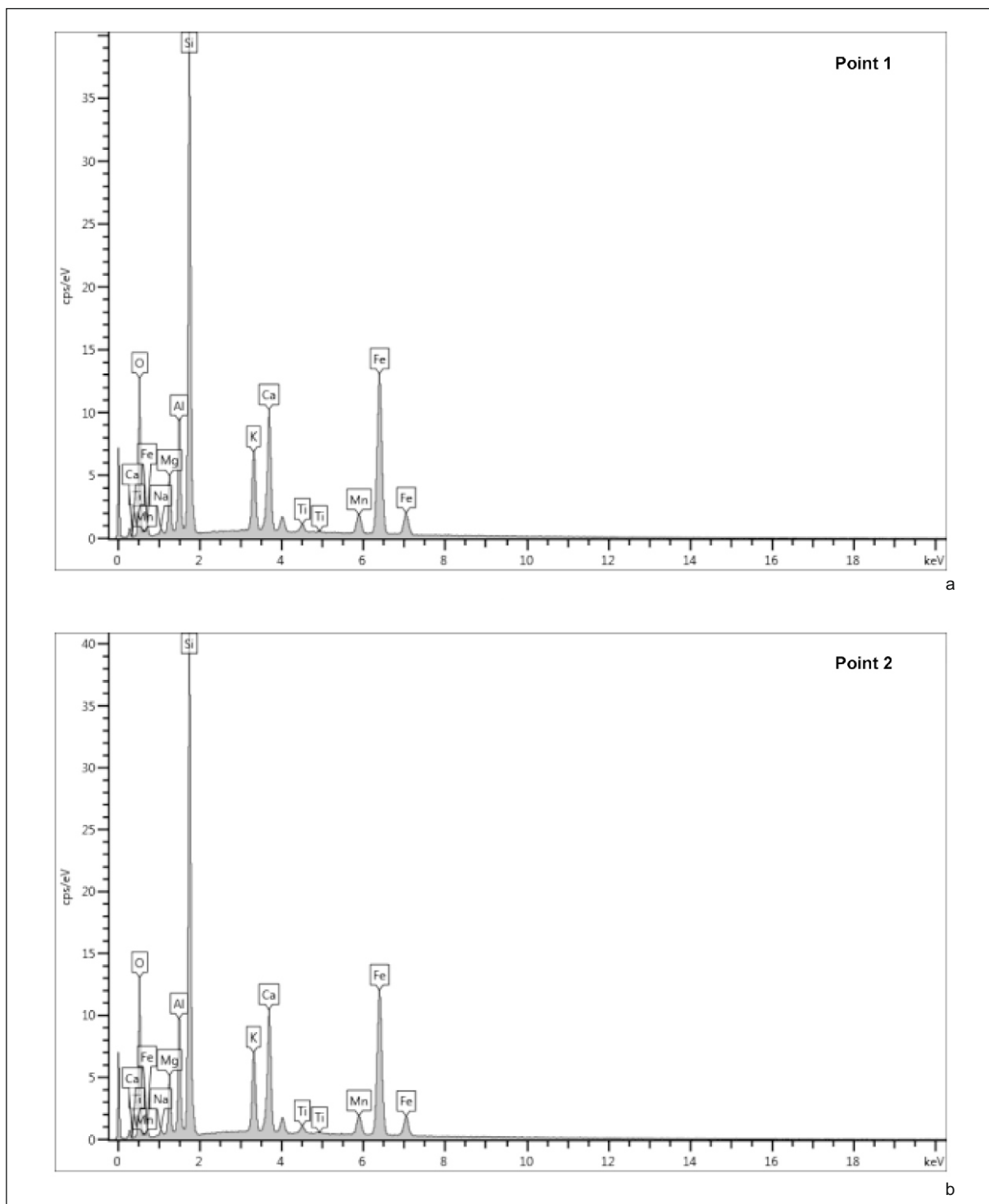


Fig. 21. EDS spectra from the analysis of the single-phase slag inclusion (SI5): a – EDS analysis spectrum in Point 1 (dark background); b – EDS analysis spectrum in Point 2 (dark background).

Ryc. 21. Spektre EDS z analizy wielofazowego wtrącenia żużla (SI5): a – spektrum analizy EDS w punkcie 1 (ciemne tło); b – spektrum analizy EDS w punkcie 2 (ciemne tło).

and 24). A similar chemical composition (but without P and S) can be found in single-phase dark and shiny fayalite-type slag inclusions (Figs. 18-23). These inclusions form evident clusters in the metal (Figs. 18:a and 22:a).

The hardness tested on the surface of the sample is 142-173 HV10 in zones with higher carbon content. In local zones with lower carbon content its value is 119 HV10 (Fig. 6:b).

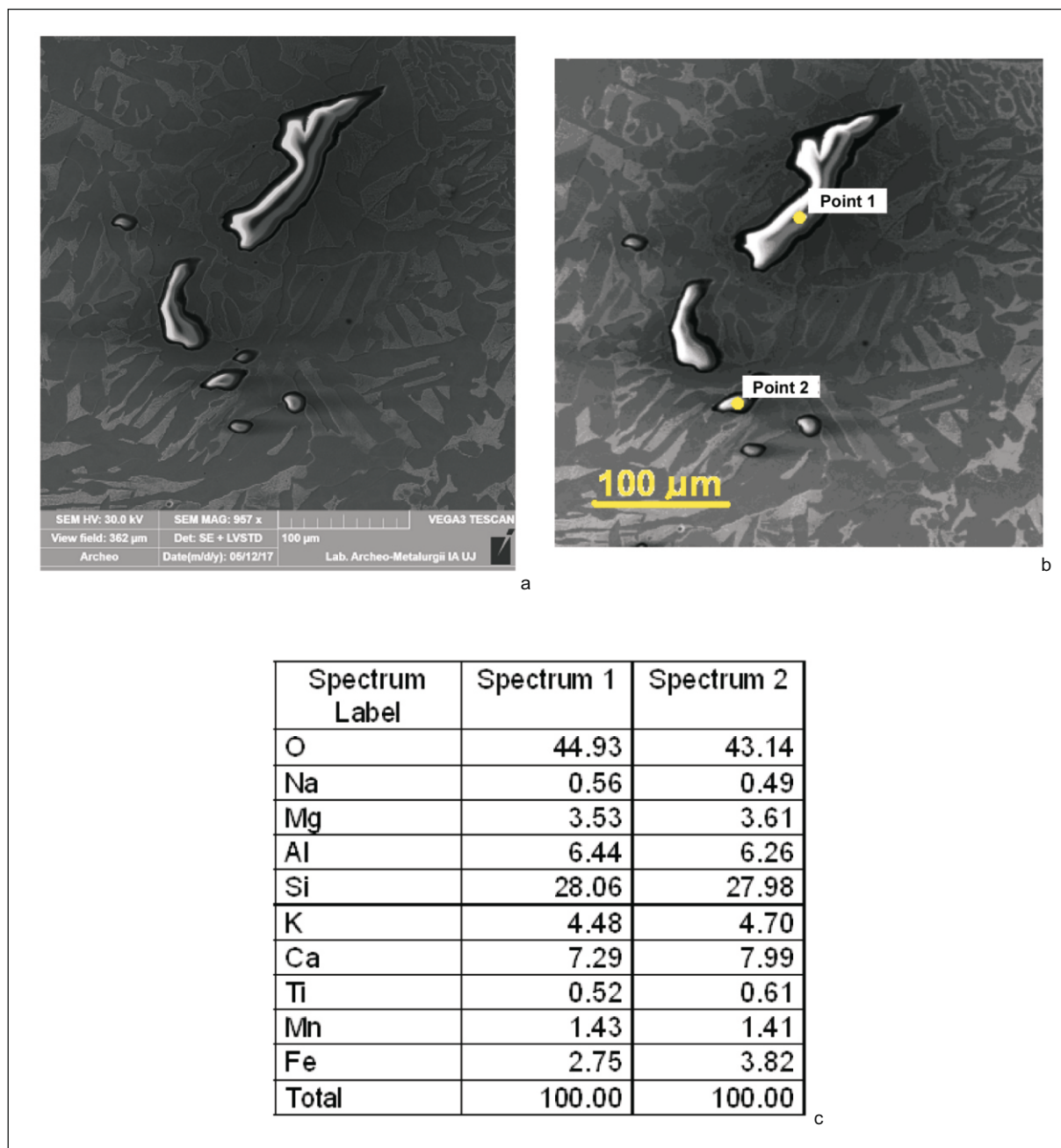


Fig. 22. Single-phase slag inclusions (SI6 – shining in the scanning microscope under the impact of electron beam) in the cross-section of the sample from the hackbut barrel, inv. No. MZM/421/MT and their EDS point analysis: a – morphology of shiny slag inclusions; b – analyses slag inclusions, Points 1 and 2 (shiny background); c – results of quantitative EDS analysis in Points 1 and 2.

Ryc. 22. Jednofazowe wtrącenia żużla (SI6 – lśniące pod mikroskopem skaningowym pod uderzeniem wiązki elektronów) na przekroju próbki z lufy hakownicy, nr inv. MZM/421/MT i ich punktowa analiza EDS: a – morfologia lśniących wtrąceń żużla; b – analizowane wtrącenia żużla, punkty 1 i 2 (lśniące tło); c – wyniki analizy ilościowej EDS w punktach 1 i 2.

### Technology of manufacture

On the basis of the metallographic examinations and the analysis of slag inclusions it can be said that the barrel was forged from semi-hard bloomery steel with 0.3-0.5% C. The presence of acicular Widmanstätten ferrite in the microstructure of the hackbut demonstrates that

the metal was overheated and thus more prone to crack. Such metal had a negative impact on utilitarian properties of the gun.

Concerning methods of manufacture of iron-forged barrels of hand-held firearms, they were forged from one or several pieces of iron on an iron core. After the tube had been made,

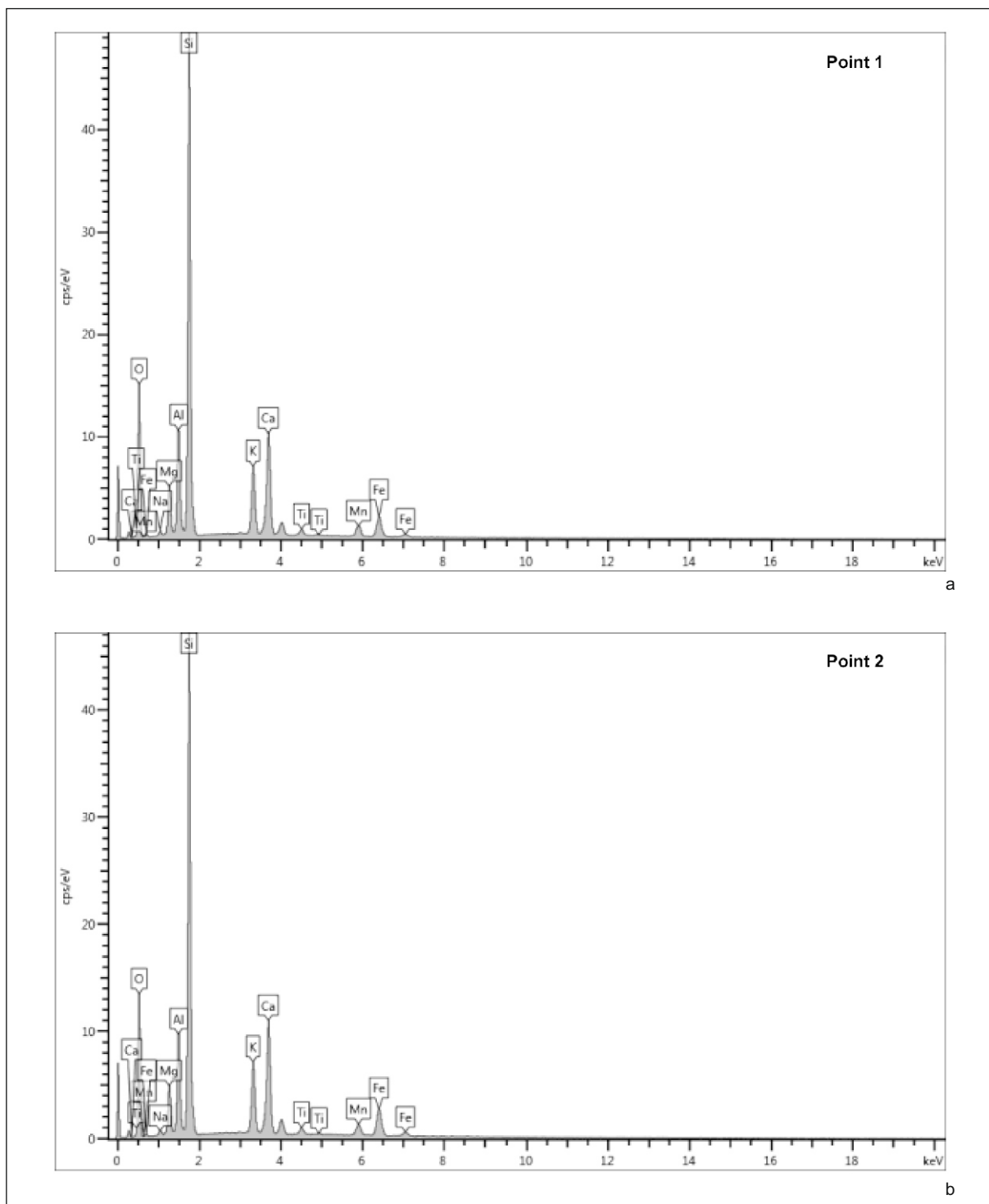


Fig. 23. EDS spectrums from the analysis of the single-phase slag inclusion (SI6): a – EDS analysis spectrum in Point 1 (shiny background); b – EDS analysis spectrum in Point 2 (shiny background).

Ryc. 23. Spekttra EDS z analizy jednofazowych wtrąceń żużła (SI6): a – spektrum analizy EDS w punkcie 1 (lśniące tło); b – spektrum analizy EDS w punkcie 2 (lśniące tło).

it was blocked in the breech part with a cylinder-shaped peg, which was then carefully forged. Hooks were manufactured separately, and then they were forge-welded to barrels. P. Strzyż remarks with right that due to a high

susceptibility to damage of early hand-held firearms, the only way to prevent barrels from bursting was to make them thick enough (Thierbach 1897-1899, 132; Szymczak 2004, 81, 100; Buchwald 2008, 285-288; Strzyż 2011, 20,

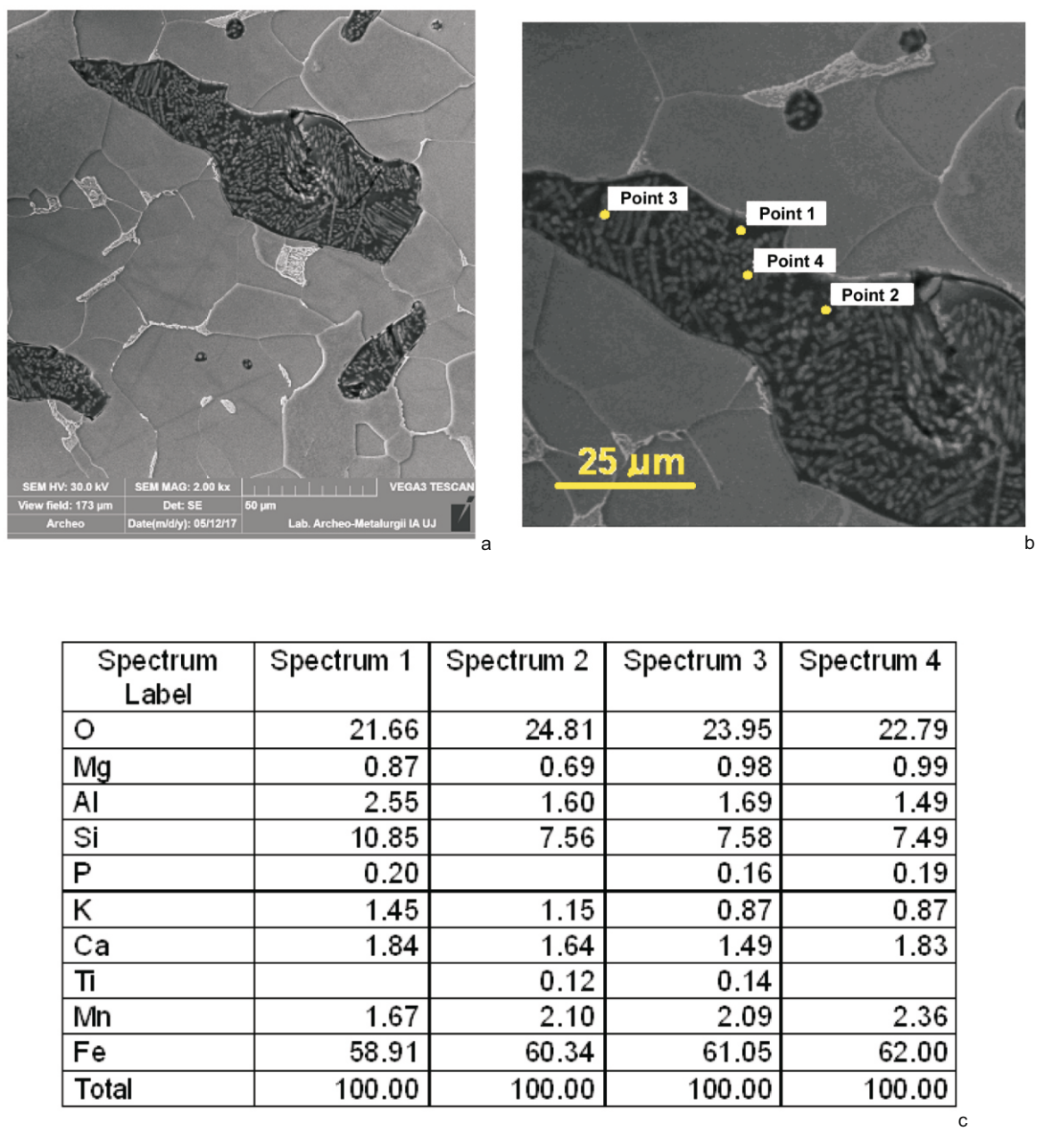


Fig. 24. Multi-phase slag inclusion (SI7) in the cross-section of the sample from the hackbut barrel, inv. No. MZM/421/MT and its EDS point analysis: a – morphology of multi-phase slag inclusions; b – analysed points in the slag inclusion: Points 1 and 2 (dark background), Points 3 and 4 (bright tiny globular particles); c – results of the quantitative EDS analysis in Points 1-4.

Ryc. 24. Wielofazowe wtrącenie żużla (SI7) na przekroju próbki z lufy hakownicy, nr inw. MZM/421/MT i jego punktowa analiza EDS: a – morfologia wielofazowego wtrącenia żużla; b – analizowane punkty na wtrąceniu żużla: punkty 1 i 2 (ciemne tło), punkty 3 i 4 (jasne drobne okrągłe cząsteczki); c – wyniki analizy ilościowej EDS w punktach 1-4.

24; 2014, 232, 234-239; Klimek et al. 2013, 94-96; on technology of wrought iron guns see also Smith 2000, 68-80; Smith, DeVries 2005, 238-239). This may also be the case concerning the discussed hackbut, as metallographic analyses demonstrated its susceptibility to damage. Interestingly, P. Strzyż says that at least

until the mid-15<sup>th</sup> century copper was more eagerly used than iron for the manufacture of hackbut barrels. The fact that most hackbut which have survived are made from iron is caused by mass re-melting of damaged or obsolete copper alloy barrels (Strzyż 2014, 47, 213-214).

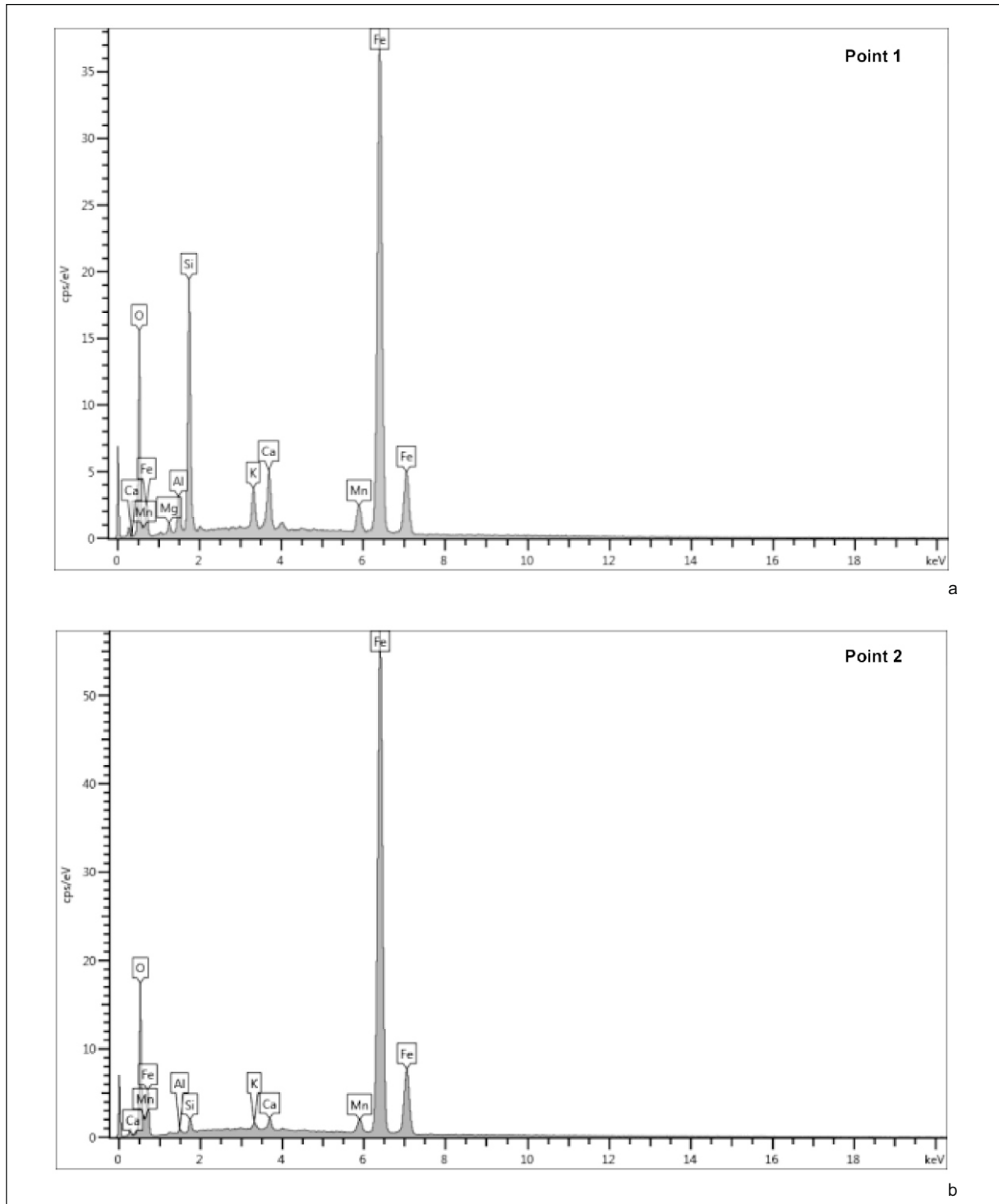


Fig. 25. EDS spectra from the analysis of the multi-phase slag inclusion (SI7): a – EDS analysis spectrum in Point 1 (dark background); b – EDS analysis spectrum in Point 2 (dark background).

Ryc. 25. Spektre EDS z analizy wielofazowego wtrącenia żużla (SI7): a – spektrum analizy EDS w punkcie 1 (ciemne tło); b – spektrum analizy EDS w punkcie 2 (ciemne tło).

With regard to other examples of hand-held firearms, the barrel of a handgunne from Ostrožská Nova Vés in Bohemia (14<sup>th</sup>/15<sup>th</sup> century) was made from iron with 99.92% Fe, 0.05% Mn, 0.08% P and 0.05% C. It was assumed that the

barrel was forged in a temperature of ca. 720° C, which caused less deformation during later slow cooling (*ibid.*, 236, Cat. No. 20; see also Figel' et al. 2010, 484-485; Klimek et al. 2013, 95).

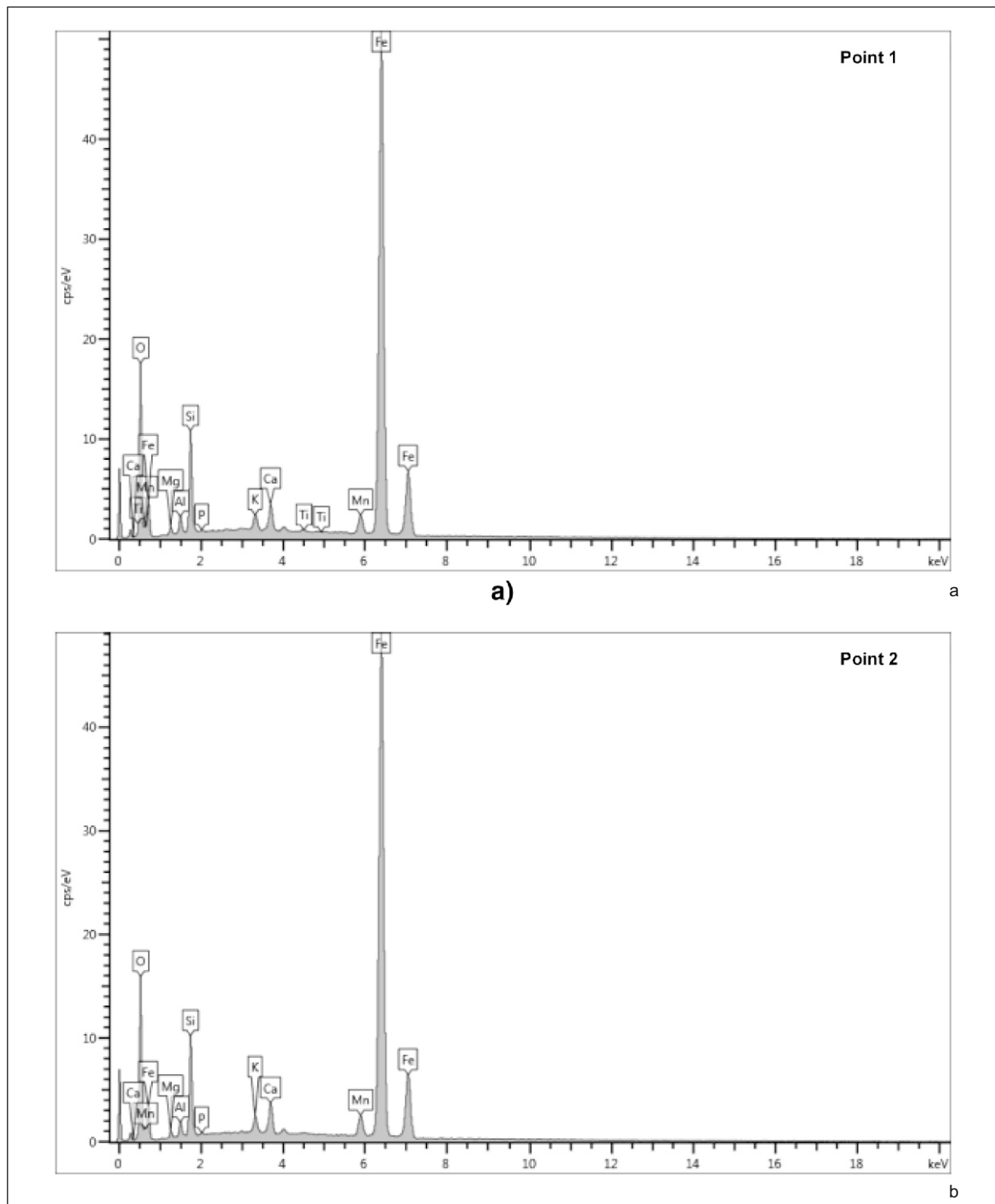


Fig. 26. EDS spectra from the analysis of bright tiny globular separations in the multi-phase slag inclusion (SI7): a – EDS analysis spectrum in Point 3; b – EDS analysis spectrum in Point 4.

Ryc. 26. Spektre EDS z analizy jasnych drobnych okrągłych wydzieleń w wielofazowym wtrąceniu żużla (SI7): a – spektrum analizy EDS w punkcie 3; b – spektrum analizy EDS w punkcie 4.

A fragment of a possible hackbut barrel from the vicinity of Křídlo Castle in Bohemia (ca. 1470s?) was made from ferritic metal. Its hardness was  $184 \pm 14$  HV0.01. The metal was

pretty clean, which was perhaps due to numerous stages of forging. This process removed much of slag (Figel' et al. 2010, 483; see also Klimek et al. 2013, 95-96; Strzyż 2014, 236-237, Cat. No. 76).

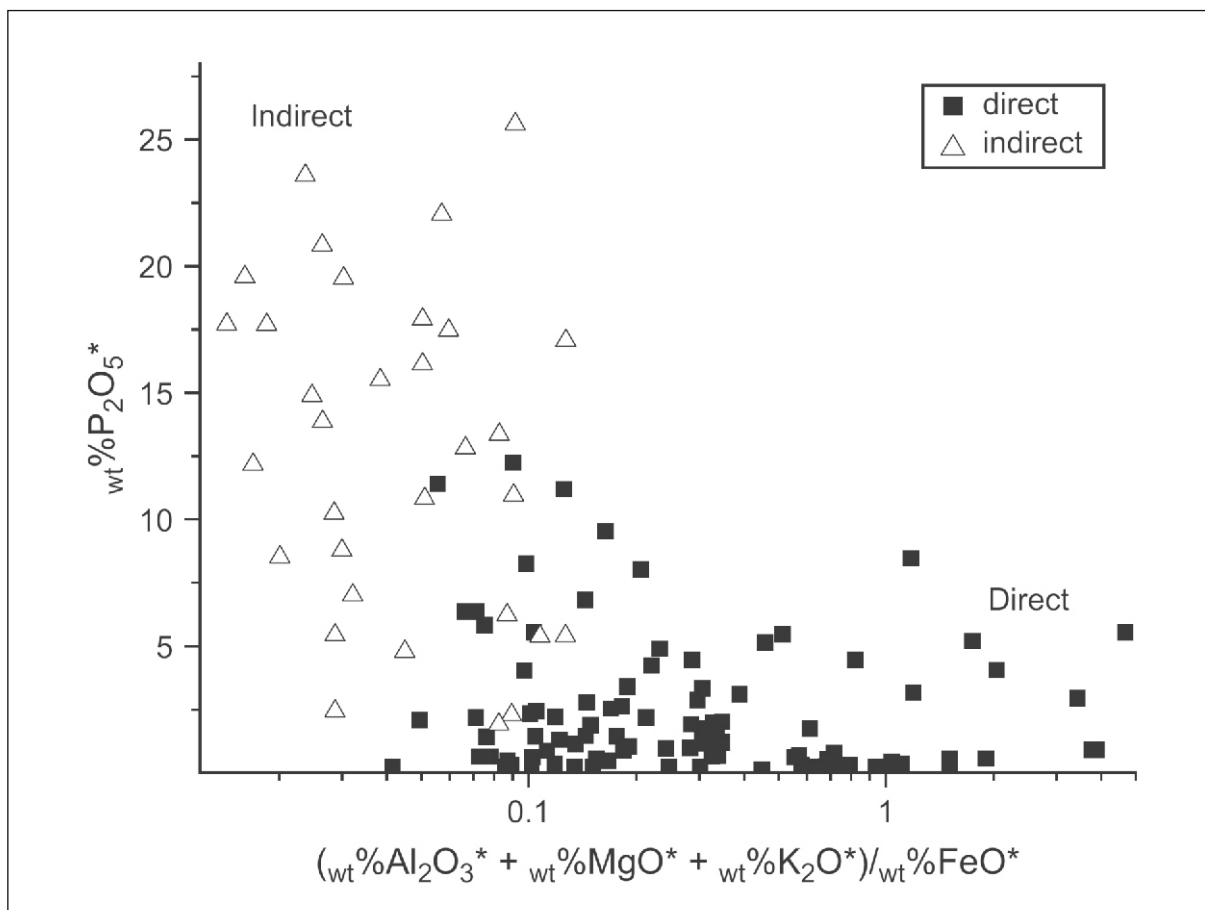


Fig. 27. Distinction between the direct and the indirect process on the basis of weighted contents of oxides (after Dillman, *L'Héritier* 2007, 1819, Fig. 10).

Ryc. 27. Rozróżnienie między procesem bezpośrednim a pośrednim na podstawie zawartości ważonej tlenków (wg Dillman and *L'Héritier* 2007, 1819, Fig. 10).

The barrel of the afore-mentioned hackbut from Helfštýn Castle was made from ferrous alloy with a high content of phosphorus. Two zones were identified in the sample. The first one was homogeneously ferritic. Its phosphorus content was 0.5-0.6% P and its hardness was 161±14 HV0.2. The other zone was ferritic-pearlitic and the carbon content was 0.2-0.3% C. As mentioned above, this weapon was burst. It was believed that the damage may have been caused both by a too high phosphorus content (it makes iron too brittle) and the fact that the barrel was forged at a too high temperature of more than 950° C. In result of the latter, it came to a diffusion of phosphorus between ferritic structures, which led to a formation of micro-cracks during the process of cooling (Figel' et al. 2010, 481-484, Fig. 9, 486-487, Figs. 10-11; see also Klimek et al. 2013, 96; Strzyż 2014, 237, cat. No. 75). Furthermore, the afore-mentioned uneven thickness of the barrel's walls may have been another factor which contributed to the damage.

Another example is offered by a hackbut from Esztergom Castle in Hungary (late 15<sup>th</sup> – early 16<sup>th</sup> century). It was made from ferritic-pearlitic ferrous alloy with the carbon content of 0.2-0.3% C. Its average hardness was about 167 HV1 (Strzyż 2014, 238, Cat. No. 146).

For the sake of comparison, some words may also be said on iron-forged artillery barrels. Samples taken from the powder chamber of the Boxted bombard (made from staves and hoops, possibly 15<sup>th</sup> century) demonstrated the presence of iron with between <0.04 and <0.1% C, and with a high content of phosphorus (up to 0.36% P). Hardness values varied between 171 and 306 HV0.1. Samples from the barrel also mainly revealed soft iron, but in one sample a zone with up to 0.6% C was identified. Furthermore, Widmannstätten structures were found. These were believed to be characteristic for medium-carbon steel subject to rapid cooling (Smith, Brown 1989, 52-62, Appendix 2, 90-93, Tab. 4, 94-95, Figs. 78-80, 97; see also Smith 2000, 75; Strzyż 2014, 233-234).

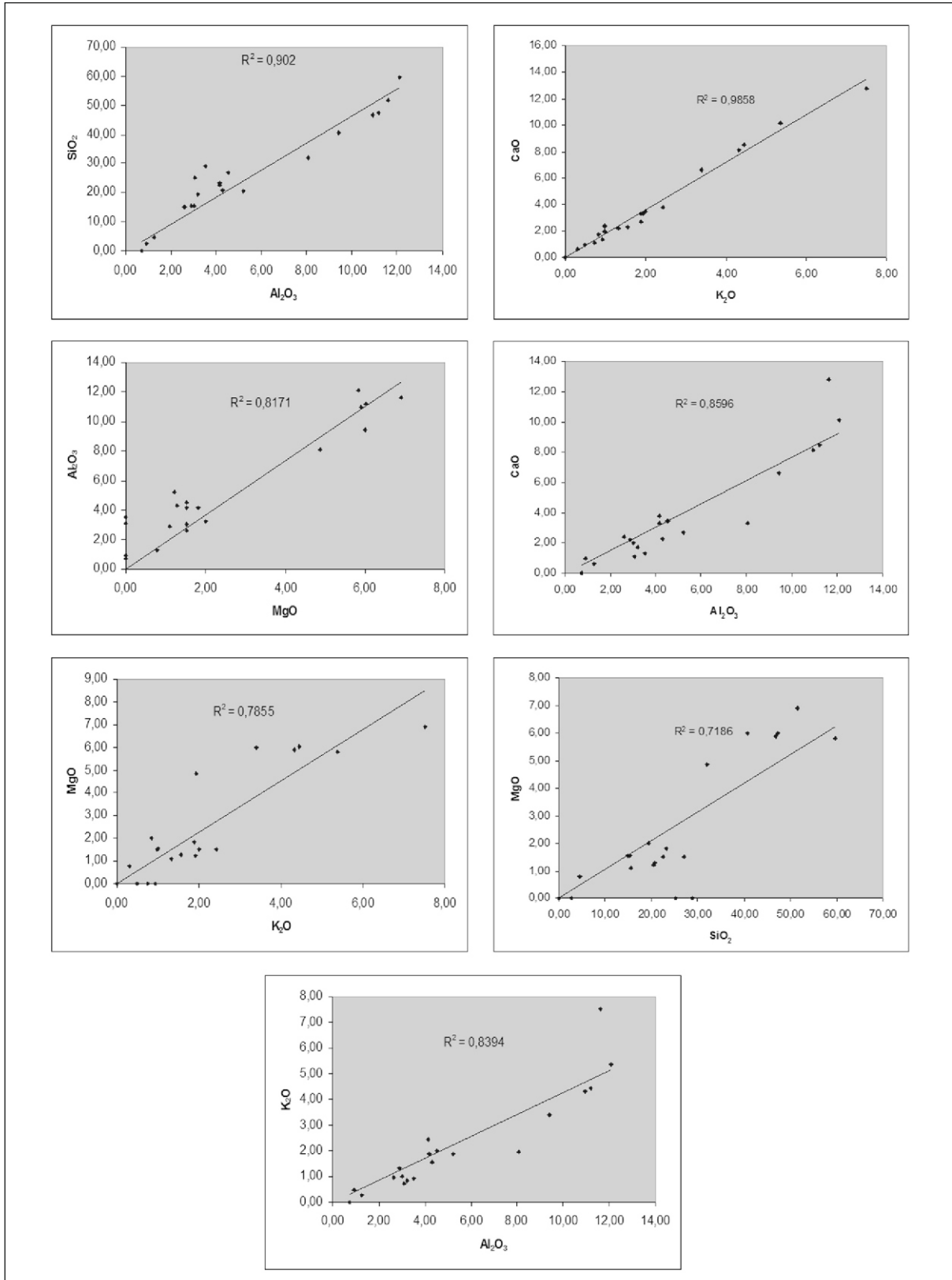


Fig. 28. Hackbut barrel, inv. No. MZM/421/MT – determination coefficients  $R^2$  of oxide ratios from Table 3.

Ryc. 28. Lufa hakownicy, nr inw. MZM/421/MT – współczynniki określoności  $R^2$  proporcji tlenków z Tab. 3.

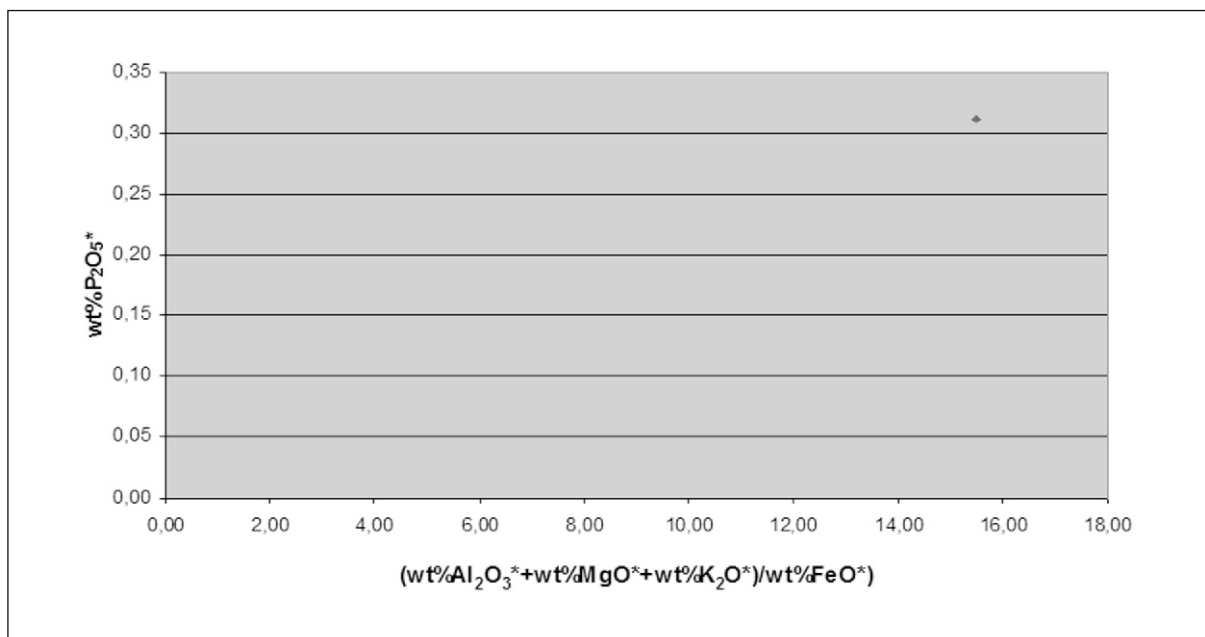


Fig. 29. Hackbut barrel, inv. No. MZM/421/MT – weighted contents\* of oxides.

Ryc. 29. Lufa hakownicy, nr inw. MZM/421/MT – zawartość ważona\* tlenków.

Wrought iron was also used for the manufacture of stave-and-hoop “Mons Meg” cannon, made in 1449. However, it was pretty heterogeneous, as the carbon content in samples from the powder chamber varied between <0.1% and 0.5% C. Hardness tests yielded results between 98 and 141 HV0.1. With regard to the barrel, the carbon content was between 0.3% and even 0.8% C, and the maximum hardness was 232 HV0.1 (Smith, Brown 1989, 1-22, Appendix 2, 90-93, Tab. 4, 94, Figs. 76-77, 96; Smith 2000, 75-76).

Another stave-and-hoop heavy cannon which was analysed with regard to its metal was “Dulle Griet” from Ghent (possibly mid-15<sup>th</sup> century). The carbon content varied between 0.05% and 0.7% C, the latter corresponding to a pearlitic-ferritic microstructure. The selection of metal may have been intentional. Steel in the barrel may have been supposed to protect it against wear caused by stone projectiles (Smith, Brown 1989, 23-38, 50, Appendix 2, 90-93, Tab. 4, 94-95, Figs. 75 and 81, 96-97; see also Strzyż 2014, 234).

Worth mentioning are also results of examinations of a late medieval stave-and-hoop cannon (U0 963 o) from the Regional Muzeum Ptuj-Ormož in Slovenia. In one of its hoops pearlitic-ferritic microstructures with 0.76% C were found, which demonstrates the use of eutectoid steel. The presence of Widmanstätten

ferrite implies accelerated cooling. It was generally assumed that the entire hoop may have been made from steel with ca. 0.5-0.6% C. The use of hard steel was explained by the fact that the hoop had had to withstand the pressure during firing of the propellant charge (Lazar 2015, 242-253).

Wrought iron, although possibly acquired in the indirect (blast furnace) process, was also the case with regard to a possibly mid-15<sup>th</sup> century cannon stored in the Museum of Artillery in Woolwich. The analysis of slag inclusions demonstrated that the content of iron in them was sometimes very low (3.60%, 3.00% and 17.80% Fe respectively). Furthermore, the content of manganese was rather high (12.90%, 13.60% and 9.20% Mn respectively; in samples from other cannons it did not exceed 5.30%). Moreover, some slag inclusions were quite globular. The carbon content in samples taken both from the powder chamber and remains of the barrel was between <0.1% and 0.2% C. Hardness values fell within the range of 117-143 HV0.1 (Smith, Brown 1989, 84-87, Appendix 2, 90-93, Tab. 4, 94, Figs. 73-73, 96, Appendix 3, Table 6, 101, 102; see also Smith 2000, 76; Strzyż 2014, 234; on cast iron and refined iron cannons see also Williams 2012, 194, 197; on cast iron in guns see also Johanssen 1918, 1-20; Buchwald 2008, 275, 323-330, 412-413, 426-427).

In the case of the stave-and-hoop Basel bombard (perhaps ca. 1420s), soft iron with

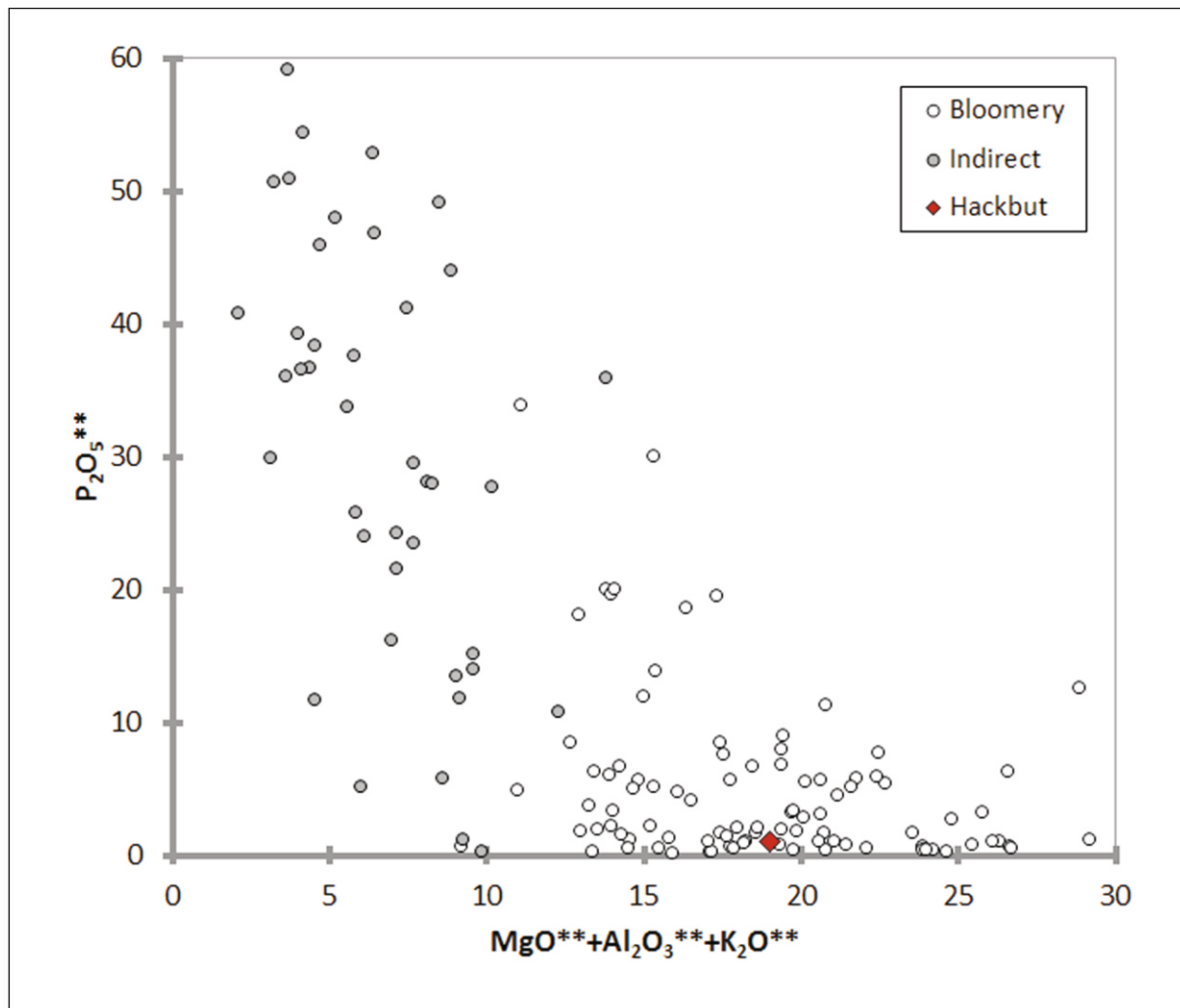


Fig. 30. Hackbut barrel, inv. No. MZM/421/MT – weighted contents\*\* of oxides against the background of comparative data. Courtesy DrMaxime L'Héritier.

Ryc. 30. Lufa hakownicy, nr inw. MZM/421/MT – zawartość ważona\*\* tlenków na tle danych porównawczych. Dzięki uprzejmości dra Maxime'a L'Héritiera.

between <0.04% and <0.1% C and an increased content of phosphorus was used. Hardness values were between 128 and 208 HV0.1 (Smith, Brown 1989, 39-45, Appendix 2, 90-93, Tab. 4, 95, Figs. 82-83, 96; see also Strzyż 2014, 234).

Soft iron was also identified in two veuglaire powder chambers from the Regional Museum in Biecz, dated to ca. 1450-1525. In the first case, a ferritic-pearlitic microstructure with an increased phosphorus content was identified. The carbon content was assessed at 0.1-0.2% C. Numerous slag inclusions imply bloomery metal. Hardness tests yielded a result of 141 HV1. In the other case, a ferritic microstructure was found with an increased content of phosphorus. The content of carbon was merely 0.022% C and the average hardness was 172 HV1. The metal was also

identified as being of bloomery origin (Klimek et al. 2013, 85-93, Figs. 5-16; see also Strzyż 2014, 234-235, Cat. Nos. 103-104).

Examinations of a possibly mid-15<sup>th</sup> century light stone cannonball cannon revealed that the barrel (assembled from staves and hoops) was made from wrought iron with numerous slag inclusions. Interestingly, the content of carbon on the internal side of the barrel was higher (0.16% C) than on the external one (merely 0.01% C). On the other hand, H. Schedelman says that this is probably incidental (Schedelmann 1939, 81-82, Fig. 2).

### Conclusions

The discussed gun is a heavy siege hackbut which may have been made in the late 15<sup>th</sup> or early 16<sup>th</sup> century. and may have remained in use

until much later. Its technology of manufacture was very typical for such guns. It was forged from semi-hard bloomery steel containing ca. 0.3-0.5% C. It seems that the manufacturer encountered certain technological problems in the course of the manufacturing process. First of all, in all probability the manufacturer was unable to secure a more or less even thickness of the barrel's walls. This may have partially been caused by forge-welding of the hook to the barrel. Furthermore, on the basis of technological examinations it can be said that the metal was overheated. It cannot be excluded that the smith may have found a thick piece of steel rather difficult to forge and decided to heat it "as hot as possible" in order to make the work easier. However, overheating and then accelerated cooling of steel led to the formation of Widmanstätten structures in the metal. All these imperfections negatively influenced functional properties of the barrel and rendered it more prone to crack. It could be supposed that manufacturers of gun barrels were aware of potential difficulties which could end disastrously for final users of guns. The best solution they could think of was to

make iron-forged barrels thick enough in order to prevent them from bursting.

*Grzegorz Żabiński PhD Habil.*  
Academy of Jan Długosz  
Institute of History  
Częstochowa

*Mateusz Biborski MA*  
Institute of Archaeology of Jagiellonian  
University  
Kraków

*Marcin Biborski PhD Habil.*  
Institute of Archaeology of Jagiellonian  
University  
Kraków

*Janusz Stępiński, PhD*  
AGH University of Science and Technology  
Kraków

*Ewelina A. Miśta-Jakubowska MA*  
National Centre for Nuclear Research Świerk  
Otwock

## Bibliography

### Archival Sources:

Castle Museum in Malbork, Arms and Armour Collection – Hackbut Barrel, MZM/421/MT (inventory card).  
*Zeugbuch*

ca. 1502 *Zeugbuch Kaiser Maximilians I*, Innsbruck, Bayerische Staatsbibliothek München, Cod. Icon. 222.

### Scholarship:

Buchwald V. F.

2008 *Iron, steel and cast iron before Bessemer*, Stockholm.

Engel B.

1900-1902 *Zwei mittelalterliche Büchsen*, *Zeitschrift für Historische Waffenkunde* 2, pp. 301-302.

Figel' D., Hložek M., Hošek J., Schenk Z., Žákovský P.

2010 *Interdisciplinární analýza roztržené železné hákovnice z hradu Helfštýn*, *Castellologia Bohemica* 12, pp. 477-488.

Forrer R.

1905 *Meine gotischen Handfeuerrohre*, [in:] *Beiträge zur Geschichte der Handfeuerwaffen. Festschrift zum 80. Geburtstag von Moritz Thierbach*, ed. K. Koetschau, Dresden, pp. 23-31.

Głosek M.

1990 *Broń palna*, [in:] *Uzbrojenie w Polsce średniowiecznej 1350-1450*, ed. A. Nadolski, Łódź, pp. 155-164.

Johanssen O.

1918 *Die Anwendung des Gusseisens im Geschutzwesen des Mittelalters und der Renaissance*, *Zeitschrift für Historische Waffenkunde* 8, pp. 1-20.

Kalmár J.

1971 *Régi magyar fegyverek*, Budapest.

Klimek L., Stępiński J., Strzyż P., Żabiński G.

2013 *Late medieval wrought iron firearms from the Museum in Biecz*, *FAH* 26, pp. 83-98.

Konieczny K.

1964 *Ręczna broń palna w Polsce w XV i XVI w.*, *Muzealnictwo Wojskowe* 2, pp. 167-237.

- Lazar T.  
2015 *Poznosrednjeveško topništvo na Slovenskem. Raziskave dveh zgodnjih topov iz Pokrajinskega muzeja Ptuj – Ormož / Late-medieval artillery in Slovenia. A study of two early artillery pieces from the Regional Museum Ptuj – Ormož*, Ljubljana.
- Mielczarek M.  
1998 *Ręczna broń palna*, [in:] *Uzbrojenie w Polsce średniowiecznej 1450-1500*, ed. A. Nowakowski, Toruń, pp. 60-64.
- Schedelmann H.  
1939 *Untersuchung einer schmiedeisernen Steinbüchse aus dem 15. Jahrhundert*, ZfHWK 41 (Neue Folge 8), pp. 81-82.
- Smith R. D.  
2000 *The technology of wrought-iron artillery*, Royal Armouries Yearbook 5, pp. 68-80.
- Smith R. D., Brown R. R.  
1989 *Bombards Mons Meg and Her Sisters*, Royal Armouries Monograph 1, London.
- Smith R. D., DeVries K.  
2005 *The Artillery of the Dukes of Burgundy, 1363-1477*, Woodbridge.
- Strzyż P.  
2011 *Broń palna w Polsce średniowiecznej. Studium archeologiczne*, Łódź.  
2014 *Broń palna w Europie Środkowej w XIV-XV w.*, Łódź.
- Šnajdrová E.  
1998 *Palné zbraně ze sbírky Národního muzea*, Praha.
- Szymczak J.  
2004 *Początki broni palnej w Polsce 1383-1533*, Łódź.
- Thierbach M.  
1897-1899 *Über die erste Entwicklung der Handfeuerwaffen*, Zeitschrift für Historische Waffenkunde 1/6, pp. 129-132.
- Williams A. R.  
2012 *The Sword and the Crucible. A History of the Metallurgy of European Swords up to the 16<sup>th</sup> Century*, Leiden–Boston.
- Маковская Л. К.  
1992 *Ручное огнестрельное оружие русской армии конца XIV-XVIII в.*, Москва

Grzegorz Żabiński, Mateusz Biborski, Marcin Biborski,  
Janusz Stępiński, Ewelina A. Miśta-Jakubowska

## PÓŻNOŚREDNIOWIECZNA LUB WCZESNONOWOŻYTNA ŻELAZNA LUF A HAKOWNICY Z KOLEKCJI MUZEUM ZAMKOWEGO W MALBORKU

### Streszczenie

Artykuł omawia lufę hakownicy przechowywaną obecnie w Muzeum Zamkowym w Malborku (nr inw. MZM/421/MT). Na podstawie cech typologicznych zabytek ten określić można jako lufę ciężkiej hakownicy wałowej, pochodzącą z okresu od końca XV do początków XVI w., acz mogła ona pozostawać w użyciu znacznie dłużej. Wykonano ją w technologii dość typowej dla tego rodzaju broni – została ona wykuta z dymarskiej stali półtwardej zawierającej około 0.3-0.5% C. Podczas wykonywania lufy wytwórca napotkał pewne problemy technologiczne. Na podstawie rekonstrukcji trójwymiarowej zabytku założyć można, iż ściany lufy hakownicy są nierównej grubości. Ponadto badania

metaloznawcze wykazały, iż metal uległ przegrzaniu podczas podgrzewania go do kucia. Zjawisko to, połączone z przyspieszonym chłodzeniem stali, skutkowało powstaniem struktur Widmanstättena w metalu. Wszystko to obniżyło właściwości użytkowe lufy, czyniąc ją podatniejszą na pęknięcie. Przyjąć można, iż wytwórcy luf byli świadomi tego problemu, a rozwiązaniem, które miało zapobiec pęknięciu podczas ich użytkowania, było wykucie luf o odpowiednio grubych ścianach.

W Aneksie do artykułu podjęto próbę weryfikacji metody wytopu metalu za pomocą analizy zawartych w nim wtrąceń żużla. Wydaje się ona potwierdzać, iż metal ten jest pochodzenia dymarskiego.

## APPENDIX

Grzegorz Żabiński  
Ewelina A. Miśta-Jakubowska

## AN ATTEMPT AT IDENTIFYING THE SMELTING PROCESS WITH THE USE OF SLAG ANALYSIS\*

It has been said in previous scholarship that it is possible to distinguish between direct (bloomery) and indirect (blast furnace and refining) smelting processes on the basis of results of slag analysis. A comprehensive approach was proposed by Ph. Dillmann and M. L'Héritier. Their point of departure was an observation that the composition of slag inclusions in an artefact results on the one hand from the composition of materials participating in the smelting process (ore, fuel, furnace or hearth lining, additives and the like) and on the other hand from the ironmaking process itself. In the direct process, such compounds as iron and phosphorus oxides are partially reduced and the content of Fe and P in slag inclusions directly depends on the efficiency of reduction. In the indirect process, it comes to an almost complete reduction of iron and phosphorus oxides to cast iron. Therefore, the final composition of slag inclusions will be influenced by refining conditions. These slag inclusions will vary a great deal. There will be inclusions almost totally composed of iron oxide, glassy inclusions with a low content of Fe, inclusions with intermediary phases such as fayalite  $\text{Fe}_2\text{SiO}_4$ , hercynite  $\text{FeAl}_2\text{O}_4$  or phosphates. On the other hand, some oxides (so-called NRCs or Non-Reduced Compounds) are not reduced in the process or become completely reoxidised at the end of it. From the point of view of the discussed processes the most interesting and best detectable NRCs are  $\text{MgO}$ ,  $\text{Al}_2\text{O}_3$ ,  $\text{SiO}_2$ ,  $\text{K}_2\text{O}$ , and  $\text{CaO}$ . If present in any component of the process (i.e., ore, furnace/hearth lining, fuel), these NRCs will also be present in slag inclusions. An important observation is that the ratio of these NRCs is in most cases relatively constant. This is the case with the ratios of  $\% \text{SiO}_2 / \% \text{Al}_2\text{O}_3$  and  $\% \text{MgO} / \% \text{Al}_2\text{O}_3$ , provided that there is a sufficient quantity of  $\text{MgO}$ . To some extent (but with a wider dispersion), this is also true for the ratio of  $\% \text{K}_2\text{O} / \% \text{CaO}$ . On the other hand, there is a clear anticorrelation in the  $\% \text{FeO} / \% \text{SiO}_2$  ratio. It is due to the fact that  $\text{SiO}_2$  is never reduced and the reduction of  $\text{FeO}$  depends on local thermodynamic conditions. Ph. Dillmann

and M. L'Héritier say that they were able to confirm constant NRC ratios in three reconstruction smelting experiments with different ores and furnaces. What is more, NRC ratios are more or less the same for most inclusions in metal from different stages of manufacture (from blooms to semi-products). Furthermore, NRC ratios were the same for two smelting operations carried out using the same ore, furnace and charcoal. On the basis of this it was concluded that the NRC ratio could be seen as a "signature" of a given system, i.e., a smelting operation using the same ore, fuel, fluxes and furnace lining (Dillmann, L'Héritier 2007, 1810-1815, Figs. 2-4).

On the other hand, it was observed that for some inclusions the NRC ratio is different than in the case of others. It may be due to a high fragmentation of inclusions and the presence of very small inclusions, which cause a local concentration effect. Furthermore, if additives are used in the forging stage, newly formed inclusions will have a different composition than slag inclusions related to the smelting phase. For instance, sand or clay additives were often used by blacksmiths. Due to this, if a given artefact underwent numerous stages of manufacture, there is a much higher chance that slag inclusions will be contaminated with forging additives. In other words, in highly processed artefacts, slag inclusions resulting from smelting may be a minority as compared to forging-related slag. In some cases, it is hardly possible to identify any constant NRC ratio. Therefore, this method works best with products which did not undergo many stages of manufacture (as, for instance, iron architectural elements analysed by Ph. Dillmann and M. L'Héritier in their paper) (*ibid.*, 1814-1815; using NRC ratios and correlations between them as a method of distinguishing between slag inclusions related to smelting and those deriving from other stages of manufacture was also mentioned by other scholars, see Charlton et al. 2012, 6; for this issue see also Blakelock et al. 2009, 1748).

Ph. Dillmann and M. L'Héritier propose the following steps in the analysis:

\* The authors are obliged to Dr Maxime L'Héritier for his kind consultation and supply of comparative data.

– metallographic observation of different zones in the sample in order to find areas with different contents of C and P and to identify possible welding lines. If slag inclusions formed by additives are present in these lines, they are to be analysed

– in order to achieve a statistically representative number of inclusions, at least 40 inclusions in each zone of interest should be analysed

– the content of the following oxides in slag inclusions is calculated: Na<sub>2</sub>O, MgO, Al<sub>2</sub>O<sub>3</sub>, SiO<sub>2</sub>, P<sub>2</sub>O<sub>5</sub>, SO<sub>3</sub>, K<sub>2</sub>O, CaO, TiO<sub>2</sub>, Cr<sub>2</sub>O<sub>3</sub>, V<sub>2</sub>O<sub>5</sub>, MnO, FeO (wt%): for each NRC ratio (usually %Al<sub>2</sub>O<sub>3</sub>/%SiO<sub>2</sub>, %K<sub>2</sub>O/%CaO, and %MgO/Al<sub>2</sub>O<sub>3</sub>) it is necessary to plot the slag inclusion's composition and fit it by a linear model passing through zero. In case the determination coefficient R<sup>2</sup> is equal to or over 0.7, it is possible to consider the ratio as constant and to assume it as a slope of a modelled line. If the determination coefficient is below 0.7 but there is still a linear behaviour for a majority of inclusions, it is possible to eliminate the erratic ones and to determine the ratio by a new linear modelling

– it is necessary to calculate a “surface weighted average composition” for all elements or oxides. This is needed to take into consideration not only NRCs, but also other elements (such as P or Fe) which do not become completely reduced or oxidised in the course of the entire process. The “surface weighted average composition” is calculated on the basis of all the inclusions from a zone of interest or from the entire artefact and the calculation is done after inclusions with abnormal NRC ratios are eliminated. The calculation of the “weighted content” takes into account the ratio between the surface area of the analysed inclusion and the total analysed surface. It is expressed with the following formula:

$$\%E^* = \sum_{i=1}^n (\%E_i \times \frac{S_i}{S_T})$$

Σ – sum

%E\* – weighted content of the considered element or oxide

%E<sub>i</sub> – mass content of the element or oxide in the i Slag Inclusion (SI)

S<sub>i</sub> – surface of the SI i where the analysis is performed

S<sub>T</sub> – total surface of the analysed SI

n – total number of inclusions

– the weighted content can be indicated with a \* (e.g., %Al<sub>2</sub>O<sub>3</sub>\*), in order to distinguish it from the normal content. It is worth noting that after the elimination of abnormal inclusions, the evaluation of the NRC ratio with the use of linear regression and with the use of the ratio of weighted contents will produce the same results (Dillmann, L'Héritier 2007, 1811, 1815-1817).

In order to distinguish between the direct and indirect processes with the use of slag inclusion composition, a number of traits is proposed. It has been observed that elements present in the system could have a different behaviour depending on the smelting process (Table 1).

There are two groups of major compounds. The first one are these containing Mg, Al, K and Ca oxides which are not reduced no matter what process is used. The second one are Fe, P and Si oxides which are more or less reduced, depending on the process. As regards weighted contents, analyses of artefacts whose smelting process (direct or indirect) was certainly known demonstrate that several elements from the first group (Al, Mg, K) can be found in large quantities in inclusions coming from the direct process, as compared to artefacts made from metal obtained in the indirect process. This can be explained by the fact that in case a given element is abundantly present in the ore, it will completely pass to the reduction slag (that is, to slag inclusions in the direct process)

Element	Direct Process	Indirect Process – Reduction	Indirect Process – Refining
Fe	(M/O)	M*	M/O
P	(M/O)	M Fe <sub>3</sub> P	(M/O)
Si	O	(M/O)	O
Mn	(M/O)**	M/O (sulfides)	O
Al	O	O	-
Ca	O	O	-
K	O	O	-
Ti	O	(M/O) (carbonitrides)	O

Table 1. Behaviour of some compounds present in the ore, charcoal and furnace lining during ironmaking processes: M – mainly or totally reduced; O – non-reduced; (M/O) – more or less reduced depending on the local conditions in the furnace (\* iron oxide content of indirect process smelting slag /French: “laitier”/ is very low /<10%/; \*\* the exact behaviour has not been studied in detail so far) (after Dillmann, L'Héritier 2007, 1816, Tab. 4).

Tab. 1. Zachowanie się niektórych związków zawartych w rudzie, węgla drzewnym i ścianach pieca w trakcie procesu wytopowego: M – zredukowane w znacznym stopniu lub całkowicie; O – niezredukowane; (M/O) – zredukowane mniej lub bardziej, w zależności od warunków lokalnych w piecu (\* zawartość tlenków żelaza w żużlu wytopowym /fr. “laitier”/ z procesu pośredniego jest bardzo niska /<10%/; \*\* dokładne zachowanie nie zostało dotychczas szczegółowo przebadane) (wg Dillmann, L'Héritier 2007, 1816, Tab. 4).

in the course of smelting. Concerning the indirect method, slag inclusions are formed in the course of refining by means of oxidisation of elements present in the cast iron. Therefore, elements which are absent in cast iron will not be strongly represented in the slag. It is of course possible that an element may be introduced in the refining hearth (for instance, CaO added to remove phosphorus from the metal). In such a case, this element will be present in slag inclusions. Therefore, Ca should not be considered as a discriminating element. Moreover, certain elements (such as Mg and K can pass to the metal from fuel (charcoal). However, if considerable amounts of these elements are present in the ore, it will be enough to make the difference between the direct and indirect processes by analysing slag inclusions.

For the second group of elements (Fe, P and Si), the amount of phosphorus in slag inclusions from the indirect process can be much higher than in slag inclusions from the direct process. In some cases it is possible to note a very high content of P in slag inclusions from the indirect process. This phenomenon is explained by a complete reduction of phosphorus oxide. Phosphorus then gathers in cast iron in the form of phosphorus eutectics and constitutes one of major elements in this alloy. In the course of refining the greatest part of P

undergoes oxidisation, which sometimes results in slag inclusions which are very rich in P. It is for this reason that slag inclusions formed in the refining hearth usually contain much more P oxides than slag inclusions from the direct process (where the content of P is of the same order of magnitude as in the ore). As regards silicon, some slag inclusions from the direct process contain higher amount of SiO<sub>2</sub> than slag inclusions formed in the indirect process. An explanation is that that Si oxides are not reduced in the direct process. Although some SiO<sub>2</sub> is reduced in the indirect process and Si is oxidised during refining, the amount of Si in refining slag is lower. For iron oxides (reduced in both processes), in the direct process, local highly reductive conditions in the course of the direct process can produce relatively Fe-poor inclusions. In contrast to that, slag inclusions which originate in the course of refining are formed in relatively oxidising conditions. Therefore, high amount of iron is oxidised in the course of pre-Bessemer refining processes (although iron oxidisation is anyway very low in comparison to oxidisation of other elements which can be found in cast iron). Due to this fact, the weighted content of iron in refining slag inclusions is always rather high.

Taking these observation into consideration, Ph. Dillmann and M. L'Héritier proposed a method

SI.test	MgO	Al <sub>2</sub> O <sub>3</sub>	SiO <sub>2</sub>	P <sub>2</sub> O <sub>5</sub>	K <sub>2</sub> O	CaO	TiO <sub>2</sub>	MnO	FeO	SO <sub>3</sub>	Na <sub>2</sub> O	Total
SI1.1	1.83	4.16	23.24	0.51	1.89	3.28	0.22	3.41	61.46	0.00	0.00	100.00
SI1.2	1.52	4.15	22.55	0.56	2.42	3.80	0.00	3.90	61.10	0.00	0.00	100.00
SI1.3	1.22	5.23	20.38	0.50	1.90	2.66	0.00	2.48	65.65	0.00	0.00	100.00
SI1.4	2.00	3.20	19.40	0.00	0.83	1.74	0.18	2.47	70.18	0.00	0.00	100.00
SI2.1	0.00	3.53	28.90	0.68	0.93	1.32	0.00	0.57	63.68	0.40	0.00	100.00
SI2.2	0.00	0.72	0.00	0.00	0.00	0.00	0.00	0.33	98.95	0.00	0.00	100.00
SI2.3	0.00	3.08	25.19	0.51	0.73	1.07	0.00	0.58	68.83	0.00	0.00	100.00
SI3.1	1.52	4.53	27.05	0.00	1.99	3.48	0.00	2.85	58.58	0.00	0.00	100.00
SI3.2	0.00	0.94	2.69	0.00	0.48	0.98	0.00	2.10	92.82	0.00	0.00	100.00
SI3.3	0.78	1.27	4.61	0.00	0.30	0.64	0.24	1.76	90.41	0.00	0.00	100.00
SI4.1	5.99	9.42	40.69	0.00	3.40	6.60	0.61	2.69	29.80	0.00	0.80	100.00
SI4.2	4.87	8.07	31.86	0.00	1.94	3.34	0.36	1.31	48.25	0.00	0.00	100.00
SI5.1	5.90	10.95	46.78	0.00	4.32	8.16	0.80	2.22	20.24	0.00	0.64	100.00
SI5.2	6.01	11.19	47.36	0.00	4.44	8.48	0.75	2.25	18.86	0.00	0.67	100.00
SI6.1	5.82	12.09	59.64	0.00	5.36	10.13	0.86	1.83	3.51	0.00	0.75	100.00
SI6.2	6.90	11.60	51.62	0.00	7.51	12.79	0.94	2.08	5.60	0.00	0.95	100.00
SI7.1	1.29	4.29	20.69	0.41	1.56	2.29	0.00	1.92	67.55	0.00	0.00	100.00
SI7.2	1.09	2.89	15.47	0.00	1.32	2.19	0.19	2.59	74.24	0.00	0.00	100.00
SI7.3	1.53	3.01	15.30	0.35	0.99	1.97	0.22	2.55	74.09	0.00	0.00	100.00
SI7.4	1.53	2.62	14.93	0.41	0.98	2.39	0.00	2.84	74.31	0.00	0.00	100.00

Table 2. Hackbut barrel, inv. No. MZM/421/MT – results of the elemental analyses of slag inclusions (SI) converted into oxides (wt%) (source: Figs. 9:c, 12:c, 15:c, 18:c, 20:b, 22:c, 24:c).

Tab. 2. Lufa hakownicy, nr inw. MZM/421/MT – wyniki badań składu pierwiastkowego wtrąceń żużła (SI) po przekształceniu na tlenki (%wag) (źródło: Figs. 9:c, 12:c, 15:c, 18:c, 20:b, 22:c, 24:c).

to distinguish between the direct and the indirect process. Wt% of  $P_2O_5^*$  are plotted on the y axis of a diagram, while the x axis displays  $(wt\%Al_2O_3^*+wt\%MgO^*+wt\%K_2O)/wt\%FeO^*$ . It can be seen that for most slag inclusions from artefacts made in the indirect process y values are high and x are low, while the reverse is true for the direct process. Of course, a sort of an overlapping zone or a “common domain” can be seen. For results falling within this zone it is impossible to distinguish between the two processes (Fig. 27) (*ibid.*, 1816-1819, Tab. 4, Fig. 10; for other works in which this method was used, sometimes with modifications, see, e.g., Maia et al. 2015; Disser et al. 2014; L’Héritier et al. 2012; for earlier attempts at distinguishing between the two processes see, e.g., Buchwald, Wivel 1998, 87-91, Tab. 4, Fig. 17).

Alternatively, it is possible to use weight percents of oxides which are divided by the content of Fe in the slag inclusions (so-called weighted contents\*\*). In this case, the diagram will display the following results:

– y axis:  $wt\% P_2O_5^{**}$ , that is,  $100 \times (P_2O_5^*)/((AllOxides^*)-FeO^*)$

– x axis:  $(wt\%Al_2O_3^{**}+wt\%MgO^{**}+wt\%K_2O^{**})$ , that is,  $(100 \times (Al_2O_3^*)/((AllOxides^*)-FeO^*))+(100 \times (MgO^*)/((AllOxides^*)-FeO^*))+(100 \times (K_2O^*)/((AllOxides^*)-FeO^*))$

The principle of discrimination, i.e., y values high, x values low for the indirect process and y values low, x values high for the direct process, remains the same (Dr Maxime L’Héritier, personal communication, 9 June 2017; see also Disser et al. 2014, 325).

In order to verify the assumption that the discussed hackbut barrel was in fact made from bloomery metal, it was decided to analyse oxides in slag inclusions with the use of the method discussed above. It must be said that initial requirements proposed by Ph. Dillman and M. L’Héritier were not completely met in this case. This was because:

– the results of the slag inclusion analysis were expressed in wt% of elements, not of oxides. Therefore, they had to be first converted into oxides, which always bears a risk of some error  
– instead of postulated results of analyses of at least 40 slag inclusions, only those for 7 inclusions were available (20 tests altogether). This obviously implies that the obtained results may not be fully representative for the entire artefact

– eventually, it is certain that the metal for the barrel was quite strongly processed after smelting, as it can be judged from a relatively low amount of slag (see Fig. 6:c-d, f-g and Fig. 7:a-d). Therefore, many slag inclusions may be related not to the smelting process itself, but to later stages of manufacture.

SI.test	Al <sub>2</sub> O <sub>3</sub> /SiO <sub>2</sub>	K <sub>2</sub> O/CaO	MgO/Al <sub>2</sub> O <sub>3</sub>	Al <sub>2</sub> O <sub>3</sub> /CaO	K <sub>2</sub> O/MgO	SiO <sub>2</sub> /MgO	Al <sub>2</sub> O <sub>3</sub> /K <sub>2</sub> O
SI1.1	0.18	0.58	0.44	1.27	1.03	12.73	2.20
SI1.2	0.18	0.64	0.37	1.09	1.59	14.82	1.71
SI1.3	0.26	0.71	0.23	1.97		16.77	2.76
SI1.4	0.17	0.48	0.62	1.84	0.42	9.70	3.86
SI2.1	0.12	0.70	0.00	2.67			3.80
SI2.2							
SI2.3	0.12	0.68	0.00	2.88			4.21
SI3.1	0.17	0.57	0.34	1.30	1.31	17.81	2.27
SI3.2	0.35	0.49	0.00	0.96			1.95
SI3.3	0.27	0.47	0.61	1.97	0.39	5.92	4.22
SI4.1	0.23	0.51	0.64	1.43	0.57	6.79	2.77
SI4.2	0.25	0.58	0.60	2.42	0.40	6.55	4.16
SI5.1	0.23	0.53	0.54	1.34	0.73	7.92	2.53
SI5.2	0.24	0.52	0.54	1.32	0.74	7.88	2.52
SI6.1	0.20	0.53	0.48	1.19	0.92	10.25	2.25
SI6.2	0.22	0.59	0.59	0.91	1.09	7.48	1.54
SI7.1	0.21	0.68	0.30	1.87	1.21	16.09	2.76
SI7.2	0.19	0.60	0.38	1.32	1.21	14.13	2.18
SI7.3	0.20	0.50	0.51	1.53	0.64	9.98	3.05
SI7.4	0.18	0.41	0.58	1.10	0.64	9.76	2.69

Table 3. Hackbut barrel, inv. No. MZM/421/MT – ratios of selected oxides (source: Table 2).

Tab. 3. Lufa hakownicy, nr inw. MZM/421/MT – proporcje między wybranymi tlenkami (źródło: Table 2).

The first stage was to convert the results of wt% of elements into wt% of oxides. The result can be seen in Table 2.

In the next stage of the analysis ratios of selected oxides were calculated (Table 3) and their determination coefficients  $R^2$  were defined (Fig. 28).

In the next step, weighted contents\* of individual oxides were calculated.

In the last step of the analysis, the sum of  $(wt\%Al_2O_3^* + wt\%MgO^* + wt\%K_2O^*) / wt\%FeO^*$  and the weighted content of  $P_2O_5^*$  were plotted on a diagram (Fig. 29).

As it can be seen, the obtained results are clearly much closer for those for the bloomery (direct) process than for the blast furnace (indirect) process. In order to verify this observation,

Sl.test	SI Surface (Si) (in $\mu m^2$ )	SI/ST	MgO*	Al <sub>2</sub> O <sub>3</sub> *	SiO <sub>2</sub> *	P <sub>2</sub> O <sub>5</sub> *	K <sub>2</sub> O*	CaO*	TiO <sub>2</sub> *	MnO*	FeO*	SO <sub>3</sub> *	Na <sub>2</sub> O*	$(wt\%Al_2O_3^* + wt\%MgO^* + wt\%K_2O^*) / wt\%FeO^*$
SI1.1	2209.26	0.03	0.05	0.11	0.63	0.01	0.05	0.09	0.01	0.09	1.67	0.00	0.00	0.13
SI1.2	2209.26	0.03	0.04	0.11	0.61	0.02	0.07	0.10	0.00	0.11	1.66	0.00	0.00	0.13
SI1.3	2209.26	0.03	0.03	0.14	0.55	0.01	0.05	0.07	0.00	0.07	1.79	0.00	0.00	0.13
SI1.4	2209.26	0.03	0.05	0.09	0.53	0.00	0.02	0.05	0.00	0.07	1.91	0.00	0.00	0.09
SI2.1	14352.05	0.18	0.00	0.62	5.11	0.12	0.16	0.23	0.00	0.10	11.26	0.07	0.00	0.07
SI2.2	14352.05	0.18	0.00	0.13	0.00	0.00	0.00	0.00	0.00	0.06	17.50	0.00	0.00	0.01
SI2.3	14352.05	0.18	0.00	0.55	4.46	0.09	0.13	0.19	0.00	0.10	12.17	0.00	0.00	0.06
SI3.1	1799.54	0.02	0.03	0.10	0.60	0.00	0.04	0.08	0.00	0.06	1.30	0.00	0.00	0.14
SI3.2	1799.54	0.02	0.00	0.02	0.06	0.00	0.01	0.02	0.00	0.05	2.06	0.00	0.00	0.02
SI3.3	1799.54	0.02	0.02	0.03	0.10	0.00	0.01	0.01	0.01	0.04	2.00	0.00	0.00	0.03
SI4.1	381.11	0.00	0.03	0.04	0.19	0.00	0.02	0.03	0.00	0.01	0.14	0.00	0.00	0.63
SI4.2	311.34	0.00	0.02	0.03	0.12	0.00	0.01	0.01	0.00	0.01	0.19	0.00	0.00	0.31
SI5.1	605.69	0.01	0.04	0.08	0.35	0.00	0.03	0.06	0.01	0.02	0.15	0.00	0.00	1.05
SI5.2	605.69	0.01	0.04	0.08	0.35	0.00	0.03	0.06	0.01	0.02	0.14	0.00	0.00	1.15
SI6.1	4690.93	0.06	0.34	0.70	3.45	0.00	0.31	0.59	0.05	0.11	0.20	0.00	0.04	6.62
SI6.2	598.49	0.01	0.05	0.09	0.38	0.00	0.06	0.09	0.01	0.02	0.04	0.00	0.01	4.64
SI7.1	4169.45	0.05	0.07	0.22	1.06	0.02	0.08	0.12	0.00	0.10	3.47	0.00	0.00	0.11
SI7.2	4169.45	0.05	0.06	0.15	0.79	0.00	0.07	0.11	0.01	0.13	3.81	0.00	0.00	0.07
SI7.3	4169.45	0.05	0.08	0.15	0.79	0.02	0.05	0.10	0.01	0.13	3.81	0.00	0.00	0.07
SI7.4	4169.45	0.05	0.08	0.13	0.77	0.02	0.05	0.12	0.00	0.15	3.82	0.00	0.00	0.07
	Sum of SI (ST) = 81162.85	$\Sigma^* =$	1.03	3.58	20.91	0.31	1.25	2.15	0.11	1.42	69.09	0.07	0.06	Sum of $(wt\%Al_2O_3^* + wt\%MgO^* + wt\%K_2O^*) / wt\%FeO^* = 15.50$
		** =	3.34	11.60	67.65	1.01	4.04	6.96	0.36	4.61		0.23	0.21	Sum of $Al_2O_3^{***} + MgO^{***} + K_2O^{***} = 18.98$

Table 4. Hackbut barrel, inv. No. MZM/421/MT – weighted contents\* of oxides in slag inclusions (source: Table 2). Surfaces of individual slag inclusions were measured on Figs. 9:b, 12:b, 15:b, 18:b, 20:b, 22:b and 24:a.

Tab. 4. Lufa hakownicy, nr inw. MZM/421/MT – zawartość ważona\* tlenków we wtrąceniach żużła (źródło: Tab. 2). Powierzchnie poszczególnych wtrąceń żużła mierzono na Fig. 9:b, 12:b, 15:b, 18:b, 20:b, 22:b i 24:a.

Dr Maxime L'Héritier plotted the results of the weighted contents\*\* on a diagram containing his own comparative data. The results are shown in Fig. 30.

### Conclusions

The analysis of the slag inclusions in the discussed hackbut barrel seems to confirm the assumption that the metal was obtained in the bloomery (direct) smelting process. Of course, due to the afore-mentioned reservations, the results of this analysis are to be treated with care. On the other hand, they suggest that the

method in question can also in some cases be of use in analyses of artefacts made from ferrous alloys which underwent a number of stages of manufacture after the smelting process.

Grzegorz Żabiński PhD Habil.  
Academy of Jan Długosz  
Institute of History  
Częstochowa

Ewelina A. Miśta-Jakubowska MA  
National Centre for Nuclear Research Świerk  
Otwock

## Bibliography

- Blakelock E., Martínón-Torres M., Veldhuijzen H. A., Young T.  
2009 *Slag inclusions in iron objects and the quest for provenance: an experiment and a case study*, *Journal of Archaeological Science* 36, pp. 1245-1757.
- Buchwald V. F., Wivel H.  
1998 *Slag Analysis as a Method for the Characterization and Provenancing of Ancient Iron Objects*, *Materials Characterization* 40, pp. 73-96.
- Charlton M. F., Blakelock E., Martínón-Torres M., Young T.  
2012 *Investigating the production provenance of iron artifacts with multivariate methods*, *Journal of Archaeological Science* 39, pp. 2280-2293.
- Dillmann Ph., L'Héritier M.  
2007 *Slag inclusion analyses for studying ferrous alloys employed in French medieval buildings: supply of materials and diffusion of smelting processes*, *Journal of Archaeological Science* 34, pp. 1810-1823.
- Disser A., Dillman Ph., Bourgain C., L'Héritier M., Vega E., Bauvais S., Leroy M.  
2014 *Iron reinforcements in Beauvais and Metz Cathedrals: from bloomery or finery? The use of logistic regression for differentiating smelting processes*, *Journal of Archaeological Science* 42, pp. 315-333.
- L'Héritier M., Dillman Ph., Arnaud S., Fluzin Ph.  
2012 *Iron? Which iron? Methodologies for metallographic and slag inclusion studies applied to ferrous reinforcements from Auxerre Cathedral*, [in:] *The World of Iron*, eds. J. Humphris, T. Rehren, London, pp. 409-420.
- Maia R. R., Dias M. S., de Farias Azevedo C. R., Landgraf F. J. G.  
2015 *Archaeometry of ferrous artefacts from Luso-Brazilian archaeological sites near Ipanema River, Brazil*, *REM. Revista Escola de Minas, Ouro Preto* 68/2, pp. 187-193.